Chapter 12

Noninvasive Electromagnetic Biological Microwave Testing

Dalia M.N. Elsheakh, Esmat A. Abdallah and Hala A. Elsadek

Additional information is available at the end of the chapter

http://dx.doi.org/10.5772/64773

Abstract

Blood glucose monitoring is a primary tool for the care of diabetic patients. At present, there is no noninvasive monitoring technique of blood glucose concentration that is widely accepted in the medical industry. New noninvasive measurement techniques are being investigated. This work focuses on the possibility of a monitor that noninvasively measures blood glucose levels using electromagnetic waves. The technique is based on relating a monitoring antenna's resonant frequency to the permittivity, and conductivity of skin, which in turn, is related to the glucose levels. This becomes a hot researched field in recent years. Different types of antennas (wideband and narrowband) have been designed, constructed, and tested in free space. An analytical model for the antenna has been developed, which has been validated with simulations. Microstrip antenna is one of the most common planar antenna structures used. Extensive research development aimed at exploiting its advantages such as lightweight, low cost, conformal configurations, and compatibility with integrated circuits have been carried out. Rectangular and circular patches are the basic shapes that are the most commonly used in microstrip antennas. Ideally, the dielectric constant ε_r, however, and other performance requirements may dictate the use of substrate whose dielectric constant can be greater. As in our prototype blood sensor, the miniaturized size is one of the main challenges.

Keywords: microstrip patch antenna (MPA), microstrip cavity resonator biosensor (MCRB), blood glucose monitoring (BGM), diabetic patients (DP), specific absorption rate (SAR), Federal Communications Commission (FCC), radio frequency (RF), Federal Drug Association (FDA), ground penetrating radar (GPR)

1. Introduction

Electromagnetic radiation consists of waves of electric and magnetic energy moving together (i.e., radiating) through space at the speed of light. Biological hazardous effects can results from the exposure to electromagnetic (radio frequency, RF). The main effect is the thermal effects that raise the temperature of the tissues exposed to the electromagnetic waves radiation. The electromagnetic energy effect could be harmful in normal routines. FCC's policies and rules regulate the exposure and absorption of RF energy by certain healthy thresholds. The SAR (specific absorption rate) is the federal standard term used to determine safety limits for usage of wireless handheld devices as mobile phones. The standard FCC limit for such devices is 1.6 W/kg of tissues (average over one gram of tissue). The FCC does not normally investigate problems of transmitting/receiving interference with medical devices such as in hospitals. However, the FDA's center for devices and radiological health has primary check for medical usage regulations.

The used blood glucose monitors nowadays require an amount of blood (its volume about 2–10 μL) and can be taken from fingertips or any other site in the human body. It is a painful measurement. Although blood glucose measurements fluctuate much more than HbA1c measurements (where HbA1c = mmol/mol), there is a strong correlation between HbA1c measurements and average glucose measurements taken over the same time period. While it has been shown that continuous monitoring systems are more effective in adjusting blood glucose to recommended levels, adolescents and young adults often have difficulty adhering to this intensive invasive treatment. For this reason, noninvasive monitoring systems would be preferred. GMS can cost several thousand dollars, and while blood monitors are relatively inexpensive, the disposable electrodes become costly over time. The noninvasive glucose monitoring techniques have been divided into the following categories: interstitial fluid chemical analysis, breath chemical analysis, infrared spectroscopy, optical coherence tomography, temperature-modulated localized reflectance, Raman spectroscopy, polarity changes, ultrasound, fluorescence, thermal spectroscopy, ocular spectroscopy, and impedance spectroscopy. Currently, monitoring blood glucose concentration is the most frequently measured through invasive techniques. The most popular noninvasive method are interstitial fluid chemical analysis, breath chemical analysis, fluorescence, ocular spectroscopy, and RF transmission.

Each type of wave has a different wavelength and corresponds to a different frequency range in the electromagnetic spectrum. This means that these wavelengths are between 1 mm and 1 m. Because of these longer wavelengths range, microwaves are more capable of penetrating through various materials [when the electric field passes through the dielectric medium, the medium has an effect on the electric field called permittivity (ε)]. Different tissues in the human body have different contents of water and hence have different permittivities since permittivity depends on water molecules, which is due to the polarization of water molecules when it exposed to an electromagnetic field. When the frequency increased the water molecules line up very slowly, which causing energy storing in the tissues.

http://dx.doi.org/10.5772/64773

The real part of the material complex permittivity indicates the energy storage of that material, while the imaginarily part is the loss tangent factor that indicates the amount of electric field energy lost when passing through the material. Fortunately, most biological materials have permeability close to that of the free space; hence, the permeability is not a concern during text involving blood glucose levels, hence allowing the tests to concentrate on measuring the change in dielectric (permittivity) properties of the material. Measuring dialectic properties can indicate indirect measures of other properties that have a relation to the molecular structure of the material.

Different tissues in the human body have different contents of water and hence have different permittivities since permittivity depends on water molecules, which is due to the polarization of water molecules when exposed to an electromagnetic field. When the frequency increased, the water molecules line up very slowly, which causing energy storing in the tissues. While the real part of relative permittivity drops off in distinct steps as the frequency increases; therefore, it experiences something called dispersion. Each dispersion region occurs at different frequency ranges and presents different effects of electromagnetic waves on the body. The interaction of the blood glucose and any dielectric material surrounding the antenna will cause a change in the antenna characteristics. This is due to the fact that all bodies have complex relative permittivities which will interact with the antenna. As one parameters of the antenna performance is the resonance frequency which can be correlated to be blood glucose concentration. It should be noted that the range of changing the glucose level is narrow in the nondiabetic as compared to the range of changing the glucose level in diabetic patients.

An antenna is a structure, usually made from a good conducing material that has been designed to have a shape and size such that it will act as an electromagnetic sensor that radiates/receives power in an efficient manner. It is a well-established fact that time-varying currents will radiate electromagnetic waves. Thus, an antenna is a structure on which time-varying currents can be excited with relatively large amplitude when the antenna is connected to a suitable source, usually by means of a transmission line or waveguide. There is an endless variety of structural shapes that can be used for an antenna. However, from a practical point of view, those structures that are simple and economical to fabricate are the most commonly used.

For many applications, the advantages of microstrip antennas outweigh their limitations. Initially, microstrip antennas found widespread applications in military systems such as missiles, rockets, aircrafts, and satellites. Currently, these antennas are being increasingly used in the commercial sector at different applications due to the reduced cost of the dielectric substrate material and mature fabrication technologies. With continued research and development and increased usage, microstrip antennas are ultimately expected to replace conventional antennas for most applications such as mobile and satellite applications, radar antennas, Wi-Fi applications, and biomedical application.

There are many researches done on how the electrical properties of the human blood and cells that human body composed of are various due to biological effects. Microwaves are appearing in biomedical engineering applications with ever-increasing frequency. They are being used for different applications as brain imaging, breast cancer detection, and blood virus detection.

A good understanding of the electromagnetic characteristics in biological materials is required to have effective models.

One of these researches for noninvasive test is to design a micro-immunosensing diagnostic assay called "microstrip cavity resonator biosensor (MCRB)," which was used for the diagnosis of enterovirus; however, the technology can then be modified for rapid, sensitive diagnosis of other viral diseases. The diagnostic method is based on the classical antigen antibody reaction; the complex antigen antibody can be diagnosed through the use of reflection coefficient, input impedance, and resonance frequency of the microstrip cavity resonator biosensor. The values of these parameters change according to changing of the electrical properties of the tested samples, such as dielectric constant, electrical conductivity, and resistivity, from case of normal sample layer to infected sample layer with antigen/antibodies embedded. Software can be developed for automatic reading, classifying, and determining the sample infection. The use of microwave biosensor for rapid detection of the viruses limits the need for sophisticated laboratory diagnostic methods that needs long time and expert scientist to perform the test. Clearly, these blood or any clinical samples diagnostic systems are required to be developed to reach small, lightweight, robust, unobtrusive design that can be mobilized in any place. It should maintain high performance in terms of reliability and efficiency. The printed antenna presents a significant miniaturization solution for such mobile systems. The antenna acts as microstrip cavity resonator biosensor (MCRB) with performance that is directly related to the biological material super imposed layer's physical properties. The antenna design for such measurement system has a tradeoff between design parameters as efficiency, bandwidth, and radiation characteristics from one side and the accuracy and sensitivity of the measurements from the other side. It is widely accepted that antenna performance is significantly affected by close proximity to the human body. One can conclude that there is a lot of nondestructive testing concerning the noninvasive electromagnetic biological testing. What have been introduced are just two examples of using nondestructive testing in biology.

Ground penetrating radar (GPR) is used for searching on the biological material underground as mummies, excavations, and water. Ground penetrating radar (GPR) is a noninvasive or nondestructive, sub-surface imaging method that has showed a lot of success in a wide range of fields regarding geological, geotechnical, hydrological, environmental, and archaeological applications. As aforementioned, GPR technique uses an antenna pair to send EM energy into the ground and then record the returning signals. Therefore, this antenna pair has a crucial importance in affecting the overall system performance. Ground penetrating radar systems need antennas that radiate efficiently over a broad range of frequencies.

This chapter is organized as follows: Section 1 introduces nondestructive tests and it includes three examples, namely noninvasive glucose monitoring technique, the microwave biosensor for rapid detection of the viruses, and the ground penetrating radar. Section 2 introduces a background about the invasive glucose monitoring techniques and some statics about the number of diabetic people all over the world and also some economic view. It also gives a glance about the noninvasive glucose monitoring techniques that have been heavily researched over the past several decades. The problem definition is presented in Section 3 and differentiating between Type 1 and Type 2 diabetics. Section 4 introduces the methodology which the relation between the permittivity and biological modeling, some measurements on simulating sugar water as well as the design of wide band and narrow band antenna analysis. Section 5 gives a study about the microstrip cavity resonator biosensor (MCRB), and it gives a clear idea about the mobile virus diagnosis system. The ground penetrating radar system is given in Section 6 together with the design and simulation of two antennas that are used with GPR, namely the quasi-Yagi antenna and the miniaturized log-periodic dipole antenna. Simulation and measurements are given in this section. Conclusions are given in Section 7, followed by acknowledgments.

2. Background

Diabetes mellitus often refer to as diabetes is a group of metabolic diseases in which a person has high blood sugar. This high blood sugar will often cause symptoms of frequent urination, increased hunger, and increased thirst. The two types that affect the general population are known as Type 1 and Type 2 diabetes. Blood glucose concentration represents the amount of sugar in the blood of the human being, and it is measured in mg/dl. Diabetic patients suffer from the body inability to control insulin production and hence have danger sugar level. This will cause danger health problems on the future of the patient. There are two types of blood sugar level, namely hypoglycemic (concentration less than 72 mg/dl) and hyperglycemic (concentration greater than 200 mg/dl) [1, 2]. The diabetic patient should measure the glucose level in blood every day.

Once on at least from economic view in 2003, the cost of treating diabetes was estimated to be $132 billion. By 2020, it is estimated that the number of people diagnosed with diabetes could rise to over 17 million, costing an estimated $192 billion [3]. While there is no cure for diabetes, symptoms are controlled through the regulation of blood glucose levels. There are several types of measurements that can be used to monitor glucose regulation. Once in the blood stream, glucose combines with hemoglobin found in red blood cells (erythrocytes) to create glycated hemoglobin. The hemoglobin will remain glycated for the life of the erythrocyte, typically 90–120 days [4]. This makes concentration measurement the best indication of average blood glucose concentration. While measurements are the best method of long-term control, self-monitoring of blood glucose levels is fundamental to diabetes care. Frequent monitoring avoids hypoglycemia, and aids in determining dietary choices, physical activity, and insulin doses. Nowadays blood glucose measurements require an amount of blood ranging from 2 to 10 μL from fingertips or any place in the patient body, and this is considered a painful measurements. While current blood glucose monitors require small amounts of blood (2–10 μL) and can be used at sites other than the fingertips, it is still a painful and tedious measurement. Although blood glucose measurements fluctuate much more than HbA1c measurements (where HbA1c = mmols/mol), there is a strong correlation between HbA1c measurements and average glucose measurements taken over the same time period [5]. In order to reduce the blood glucose level of a patient to the recommended level, continuous monitoring system should be done. This intensive treatment is very difficult to patient, which is the reason for searching about a noninvasive monitoring technique. On the other hand, the mummy's container (cartonnage, coffin, or sarcophagus) or on linen wrappings and included papyrus scrolls in sometimes contain biological bodies.

2.1. Invasive glucose monitoring techniques

Current glucose monitoring devices are extremely similar to the devices originally created in the 1960s. Aside from the miniaturization, ease of use, and the ability to log data, the measurements fundamentally are the same as the first laboratory sensors. There are several downsides to the current offerings of glucose meters. The blood meters require a blood sample, which is a painful procedure. CGMS can cost several thousand dollars, and while blood monitors are relatively inexpensive, the electrodes are disposable and become costly over time. A single-use blood electrode strip costs about 2$, and a CGMS 3–7 day sensor can cost 30–35$ as shown in **Figures 1** and **2**.

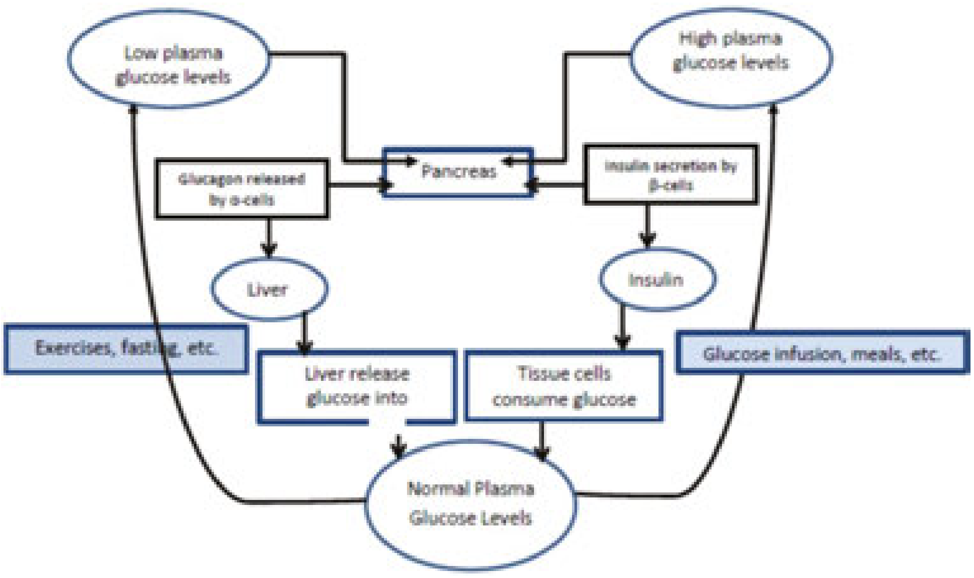

Figure 1. Typical blood glucose control system and simplified glucose measurement method.

Figure 2. Life scan OneTouch Ultra glucose meter (left), and Medtronics CGMS (right).

http://dx.doi.org/10.5772/64773

2.2. Noninvasive glucose monitoring techniques

Noninvasive glucose monitoring techniques have been heavily researched over the past several decades. They have been divided into the following categories: interstitial fluid chemical analysis, breath chemical analysis, infrared spectroscopy, optical coherence tomography, temperature-modulated localized reflectance, Raman spectroscopy, polarity changes, ultrasound, fluorescence, thermal spectroscopy, ocular spectroscopy, and impedance spectroscopy. Currently, monitoring blood glucose concentration is the most frequently measured through invasive techniques. Noninvasive blood glucose monitors offer a solution to measure proper blood glucose levels without puncturing the skin.

The following have been noninvasive; non-RF techniques have been tried [5–8]:

2.2.1. Interstitial fluid chemical analysis [9]

This technique is similar to the traditional monitoring methods since it needs the patient to switch out disposal pads for each measurement. It depends on the interaction between the enzyme and the fluids excreted from the skin. A product appeared in the market in the form of a watch using the interstitial fluid chemical analysis.

2.2.2. Breath chemical analysis [10]

It measures the level of acetone from a breath. Higher levels of acetone have been correlated to higher levels of blood glucose concentration. This method is, however, not as accurate as traditional blood glucose meters.

2.2.3. Fluorescence [11]

It is radiating from the skin and can track the level of blood glucose. The skin tissue is excited using an ultraviolet laser, and fluorescence is emitted at 380 nm. The intensity of the fluorescence can be correlated to a glucose level.

2.2.4. Ocular spectroscopy [12]

The contact lens interacts with the tears from an eye as the contact lens is illuminated by a light source; the color of the reflected light can be correlated with a blood glucose concentration. It shows promising returns.

2.2.5. RF transmission [13]

It uses two antennas to monitor blood glucose concentration noninvasively. Two matched antennas transmit and receive in a two port measurement. The transmission occurs between 5.3–5.5 GHz. The test was performed on a water-glucose solution to mimic testing on a human.

3. Problem definition

Healthcare expenditures whether by the health system or the patents reached 11% of the total healthcare in the word in 2011 (141 billion US$). Most of the countries spend between 5% and 18% of their total healthcare expenditures on diabetes. As regard Egypt, the mean healthcare expenditures was 175 US $/diabetic patient. Because of the seriousness and variability of the disease, regular testing for diabetics is required where number of tests per person vary from one to four times each day. Test strips used in daily testing are relatively expensive, costing around $1.00 per strip [4]. Over a year of testing at average twice per day, the patient will spend $730 on test strips alone and in 2020 an estimated 17.4 million people will be diagnosed with costs near $192 billion [4]. Due to the increase in the population with diabetes and the increase in the costs in treating diabetes, it is fast becoming necessary to develop new ways to test diabetes that are noninvasive, less expensive, and easy to use at home. Diabetes mellitus, more commonly known only as diabetes, is "a disease in which the body does not produce or properly use insulin" [5]. About 90–95% of the diabetes patients are of Type2 diabetes. This is characterized from the hyperglycemia which is due to impaired insulin utilization together with the body's inability to compensate increased insulin production. About 5–10% of diabetes patients are of Type 1 diabetes, which is the most dangerous type. It occurs during childhood and adolescence. It happens due to a severe deficiency of insulin secretion resolution resulting from atrophy of the islets of langerhans [5–6].

Developments for noninvasive techniques to measure blood glucose level come from the fact that Type 1 diabetics should test two times daily, and even four to six times may be required for proper monitoring in order not to result in life threatening due to misusage to insulin.

All invasive blood glucose monitors require the user to prick a finger, palm, or forearm with a lancet so that a small droplet of blood can be collected. These devices use electrochemistry of the testing strip to determine glucose levels. Each strip contains 10 layers of spacers and chemicals, including glucose oxidase and microcrystalline potassium ferricyanide. The ranges vary between meters, and the readings are not linear over the entire range; therefore, readings that are either very high or very low are open for interpretation and need to be confirmed by repeated measurements or measurements taken by a different meter [14]. According to the FDA, the goal of all future self-monitoring blood glucose systems should be able to achieve a variability of 10% at glucose concentrations of 30–400 mg/dL 100% of the time. With current systems, measurements should be within 15% of a minimally invasive method which is one that does not use subcutaneous sampling or sensors in fatty tissue to collect blood. Instead it uses percutaneous needles or sensors in the dermal layer where there are less nerve endings at sites other than the fingers to collect or react with interstitial fluid or blood. However, there are no FDA approved minimally invasive devices with sensors or sampling probes for continuous monitoring [15]. Noninvasive methods require no puncturing of the skin for testing purposes.

4. Approach and methodology

Microwaves occupy the frequencies in the electromagnetic spectrum ranging from 300 MHz to 300 GHz, which represents different types of waves. Some of the most common types of waves encountered are radio waves, UHF waves, microwaves, infrared rays, visible light, and X-rays. Each type of wave has a different wavelength and corresponds to a different frequency range in the electromagnetic spectrum [15]. The wavelengths of microwaves can be determined by the equation.

$$\lambda = \frac{C}{f} \tag{1}$$

where C is the light velocity in free space = 3×10^8 m/s.

This means these wavelengths are between 1 mm and 1 m length. Because of these longer wavelengths, microwaves are more capable of penetrating through various materials. Most measurement tools used today tend to only be able to measure wavelengths up to 50 GHz.

4.1. Material's parameters

All materials molecules have charged particles when applications of electric or magnetic field on the material, secondary field are produced which results in conduction, polarization, or magnetization of the particles. Polarization of particles results in the material acting as a dielectric which can be characterized by dielectric constant. The material relative permittivity is the ratio between the material permittivity and the permittivity of the free space. It is experimentally measurable parameters.

$$\varepsilon_r = \frac{\varepsilon}{\varepsilon_o} \tag{2}$$

When an electric field is applied across a conducting medium, an equation for complex permittivity has to be used.

$$\varepsilon = \varepsilon' - j\varepsilon'' \tag{3}$$

The real part of the complex permittivity is the dielectric constant (relative permittivity) of a material, or the energy storage of that material. The imaginary part is the loss factor, or the amount electric field energy lost when passing through a material [16]. Most biological materials have permeability close to that of free space, so permeability is not a concern during tests involving blood glucose levels, allowing the tests to focus on the frequency variations of the relative permittivity [17, 18]. Measuring the dielectric properties of a material can indirectly measure other properties that have a correlation to the molecular structure of the material [19].

Because the dielectric properties of a material are dependent upon its molecular structure, a change in the molecular structure will cause the dielectric properties of the material to change. Measuring the dielectric properties of a material can indirectly measure other properties that have a correlation to the molecular structure of the material. This can be important when the property of interest is difficult to measure directly. Most measurements involving microwaves and permittivity are taken using a vector network analyzer, or VNA. A VNA is a device that is used to measure the S-parameters of a microwave circuit over a specified frequency range and is pictured in **Figure 3**.

Figure 3. Vector network analyzer.

When an electric field is applied along conducting medium, the complex permittivity equation has to be used. Where the real part is indicates the material permittivity. In biological field, as mentioned earlier, permeability is near free space which means that the dielectric constant would be the parameter that has direct effect on frequency variation hence material properties that could be important for biological analysis.

S-Parameters: well known as scattering parameters that are used to describe completely reflection and transmission properties of a traveling wave that is scattered or reflected when a network under test is inserted into a transmission line with certain characteristic impedance.

DAK: dielectric assistive kit that is used to measure the dielectric properties of material, conductivity, permittivity, and loss tangent with high precision. **Figure 4** shows the dielectric problem designed for fast precise and nondestructive measurements of solids liquids and semisolids properties over wide frequency range, and the probe can be moved to the media under test to directly measure the dielectric parameters, thus eliminating phase distributions due to cable movements.

This open-ended coaxial probe uses advanced algorithms and novel hardware to measure the dielectric properties of liquids, solids, and semi-solids over a broad range of parameters. The measurement method is fast and nondestructive to the material under test.

Microwaves in medical applications have been making large steps in recent years since microwave technology, such as ultrasounds, allows doctors to see inside of the body without the ionizing radiation found in x-rays. To better understand how microwaves can be used in

http://dx.doi.org/10.5772/64773

medical applications, it is important to understand how microwaves affect and interact with the body.

Figure 4. DAK.

4.2. Permittivity and biological modeling

The effects of RF on biological tissues depend on the exposed field strength or the power deposited on the unit mass of these tissues. **Figure 5** shows the change in the permittivity of the human tissues due to change in the applied frequency. This effect is clear on water molecules (which are the most abundant molecules in the human body) as shown in **Figure 5**, hence, the applying field cause the water molecules to be stored in the tissues.

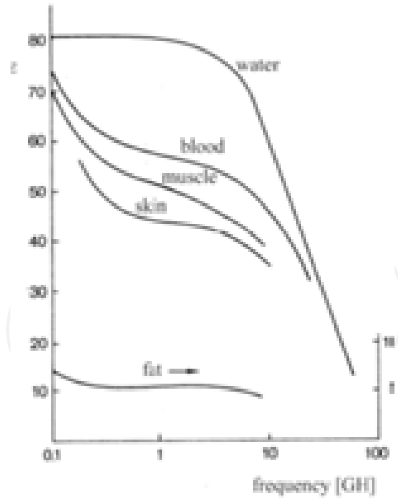

Figure 5. Dielectric constant versus frequency for different biological tissues.

Thus, the tissues do not allow energy to pass through and permittivity decrease with frequency increase.

The real part of relative permittivity drops off in distinct steps as the frequency increases; therefore, it experiences something called dispersion, which is reflected in **Figure 6** [19]. Each dispersion region occurs at different frequencies and represents different effects of electromagnetic waves on the body.

$$\hat{\varepsilon}(\omega) = \varepsilon_{\infty} + j\frac{\Delta\varepsilon}{1 + j\omega\tau} \tag{4}$$

Since biological tissues are complex in both structure and composition, and distribution parameters have to be taken into account. As a result, the second-order Debye equation is formed [11].

$$\hat{\varepsilon}(\omega) = \varepsilon_{\infty} + \sum\nolimits_{n}^{2} j\frac{\Delta\varepsilon}{1 + j\omega\tau} \tag{5}$$

where ε_{∞}, $\Delta\varepsilon$, τ are the optical permittivity, pole amplitude, and the relaxation time, respectively.

The interaction between antenna and any biological material effects on the antenna electrical properties; this effect occurs due to the complex permittivity of the biological material surround the antenna; blood is biological dielectric that subject to complex permittivity equation that depends on operating frequency range.

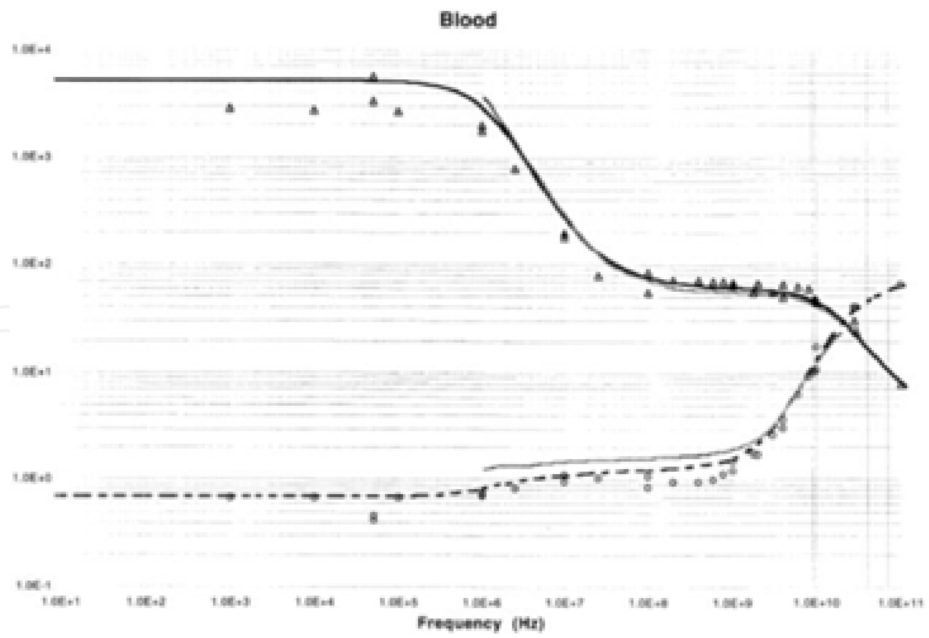

Figure 6. Permittivity and conductivity versus frequency.

Gobriel and et al [23] have analyzed the blood properties and discussed how its permittivity and conductivity changes with frequency. It is important to keep permittivity constant or semi constant in the test region; hence, we target to monitor the changes in blood permittivity due to glucose level changes.

Certain regions of dielectrics are subject to Debye and more refined Cole-Cole models. The Debye is often used for dispersions because it can contain multiple terms to describe the differing sections of the model [12], Eqs. (5) and (6).

$$\text{Debye}\,\hat{\text{m}}\text{ode}: \varepsilon(\omega) = \varepsilon_\infty + \sum_{m=1}^{n} j\frac{\Delta\varepsilon_m}{1 + j\omega\tau_m} + \frac{\delta_i}{j\omega\varepsilon_o} \tag{6}$$

$$\text{Cole-Colemodel}: \hat{\varepsilon}(\omega) = \varepsilon_\infty + \sum_{n}^{2} j\frac{\Delta\varepsilon_m}{(1 + j\omega\tau_m)(1-\alpha_m)} + \frac{\delta_i}{j\omega\varepsilon_o} \tag{7}$$

In [13], it has been determined that Cole-Cole analysis model is the best that describes the complex permittivity change of blood with frequency range. Proper curve fitting technique can be added to the Cole-Cole model to illustrate the relation between change of the blood sample permittivity with frequency and glucose level in it by [12], and the glucose factor was added by researchers [13]. An inverse relationship between dielectric permittivity and blood glucose concentration has been determined [14] as shown in **Figure 7**. The investigation was completed used an aqueous glucose solution and measured a changing glucose level and changing permittivity level over time. The change in blood glucose concentration is narrow because the patient is nondiabetic and does not experience the range of blood glucose levels that a diabetic patient experiences. It is a well–established fact that time-varying currents will radiate electromagnetic waves. Thus, an antenna is a structure on which time-varying currents can be excited with relatively large amplitude when the antenna is connected to a suitable source, usually by means of a transmission line or waveguide. There is an endless variety of structural shapes that can be used for an antenna. However, from a practical point of view, those structures that are simple and economical to fabricate are the most commonly used. In order to make antenna work adequately efficiently, the minimum size of the antenna must be comparable to wavelength [15].

Microstrip antenna is one of the most common planar antenna structures used. It has advantages such as lightweight, low cost, conformal configurations, and compatibility with integrated circuits. For many applications, the advantages of microstrip antennas outweigh their limitations. Initially, microstrip antennas found widespread applications in military systems such as missiles, rockets, aircrafts, and satellites. Currently, these antennas are being increasingly used in the commercial sector at different applications due to the reduced cost of the dielectric substrate material and mature fabrication technologies. With continued research and development and increased usage, microstrip antennas are ultimately expected to replace conventional antennas for most applications such as mobile and satellite communications, radar antennas, Wi-Fi applications, and biomedical application [20, 21].

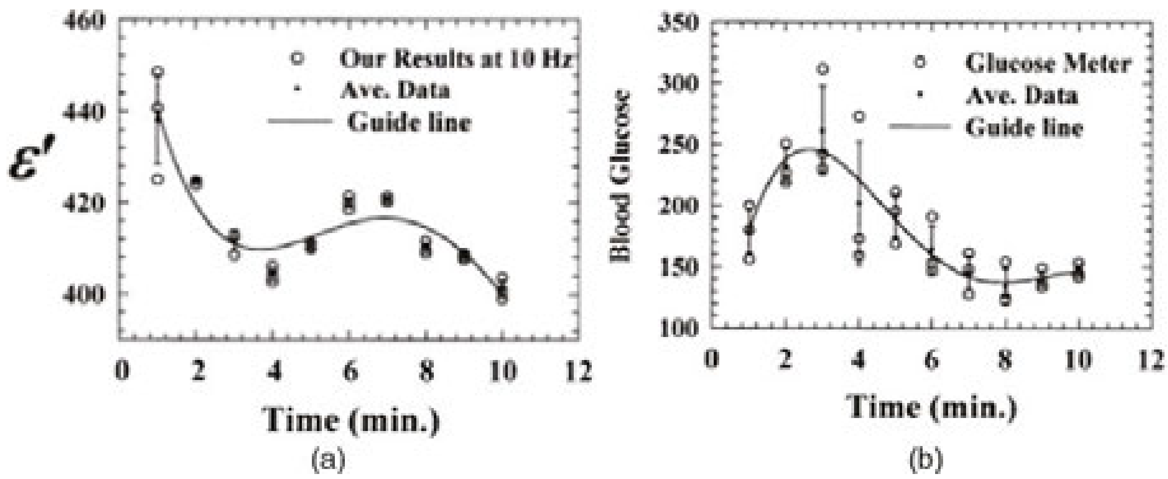

Figure 7. (a) Changes in dielectric versus (b) changes in blood glucose concentration.

This research will represent a revolution in the field of designing tests for the screening of substances of human origin with three main achievements over the available methods:

a. The instant results of screening tests on time.

b. No need for well-trained personnel or sophisticated laboratory equipment.

c. The test can be done anywhere as the device will be a portable system.

As discussed earlier, when a biological material is introduced into a resonant cavity, the cavity field distribution changes; hence, consequently, the input impedance and resonant frequencies are changed. This may depend also on the properties of electromagnetic wave input signal to the cavity as amplitude, shape, and phase. Dielectric material interacts only with electric field in the cavity. According to the theory of cavity perturbation, the complex frequency shift is as follows [3]:

$$\frac{-\partial\Omega}{\Omega}=\frac{\left(\varepsilon_r'-1\right)\int_{v_s}E.E_o^{*}dV}{2\int_{v_c}\lfloor E\rfloor^2 dV} \tag{8}$$

$$\frac{\partial\Omega}{\Omega}\approx\frac{d\omega}{\omega}+\frac{j}{2}\left[\frac{1}{Q_s}-\frac{1}{Q_o}\right] \tag{9}$$

In the above equations (Eqs. (8) and (9)), ε'_r is the real part of the relative complex permittivity associated with the dielectric loss of the material. V_s and V_c are corresponding volumes of the sample and the cavity resonator, respectively. The conductivity can be related to the imaginary part of the complex dielectric constant by separating real and imaginary parts results in Eqs. (10) and (11).

$$\varepsilon_r' - 1 = \frac{f_o - f_s}{2f_s}\left(\frac{V_c}{V_s}\right) \tag{10}$$

$$\varepsilon_r'' - 1 = \frac{Q_o - Q_s}{Q_o Q_s}\left(\frac{V_c}{4V_s}\right) \tag{11}$$

$$\sigma_e = \omega\varepsilon'' = 2\pi f \varepsilon_o \varepsilon_r'' \tag{12}$$

where f_o, Q_o, and ε''_r are operating frequency, and quality factor Q_o are corresponding to values at empty sample holder, while f_s and Q_s are same values but with filled sample holder and imaginary parts of the relative complex permittivity. The low profile, lightweight, and low manufacturing cost of microstrip patch antennas (MPA) have made them attractive candidate for this application.

4.3. Measurements on a glucose simulating sugar water

Early testing and analysis focused on looking for a shift in resonant frequency of the antenna. Modeling the shift of blood glucose concentration in the human body model using Computer simulation technology (CST) or high-frequency structure simulation (HFSS) simulators showed that the resonant frequency of the antenna would shift. Modeling the blood permittivity change with the change in its glucose level can easily lead to the change in the antenna resonance frequency. The simulation in **Figure 8** shows how the resonant frequency of the dipole antenna changes with increasing the concentration of glucoses in blood sample. As the glucose concentration increases, the antenna input impedance (real and imaginary) parts shifts. However, the real part maximum point does not lay with the imaginary part zero value; that is, these two points should lie together according to ideal theory. In such case, the resonance frequency is considered as the frequency at which the input impedance imaginary part equals zero. **Figure 9** presents how the resonance frequency increases with the increase in blood glucose concentration. On the other hand, same **Figure 9** shows that the magnitude of the antenna return loss does not show a correlation between the resonant frequency and the glucose concentration level.

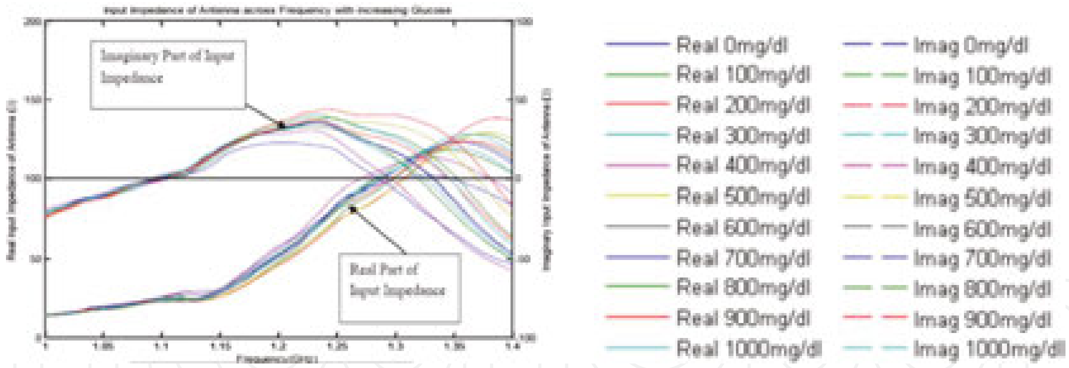

Figure 8. Simulated real and imaginary input impedance of antenna versus frequency for different glucose levels.

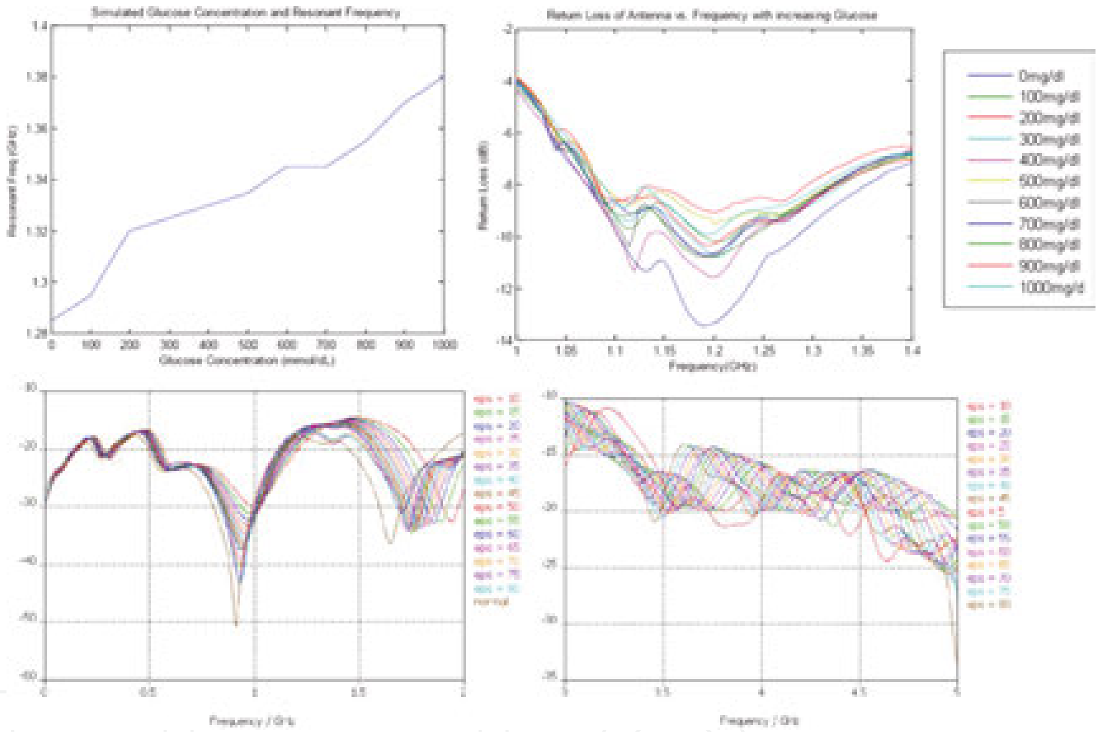

Figure 9. Resonate frequency of antenna versus glucose concentration of aqueous solution and return loss of antenna versus frequency for different glucose levels.

4.4. Design of a wideband antenna

Our proposed method would involve an antenna which would change resonant frequency based on the dielectric properties of the tissues present in its fringing fields (**Figure 10**). A similar method has been used previously by this research group to effectively characterize tissue dielectric properties [12–14]. **Figure 11** shows the measured resonant frequency of antenna vs. blood glucose levels. Modified UWB antenna return loss for varying glucose concentrations is shown in **Figure 12**. Where g is blood glucose from 70 to 150 mg/dL, and the model is defined by **Table 1**.

http://dx.doi.org/10.5772/64773

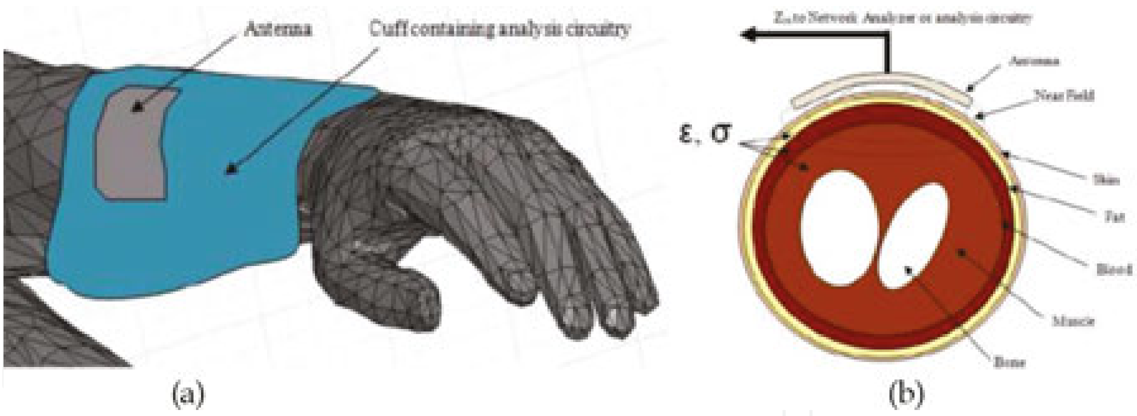

Figure 10. (a) Conceptual blood glucose measurement form factor and (b) detection of tissue properties through antenna fringing field.

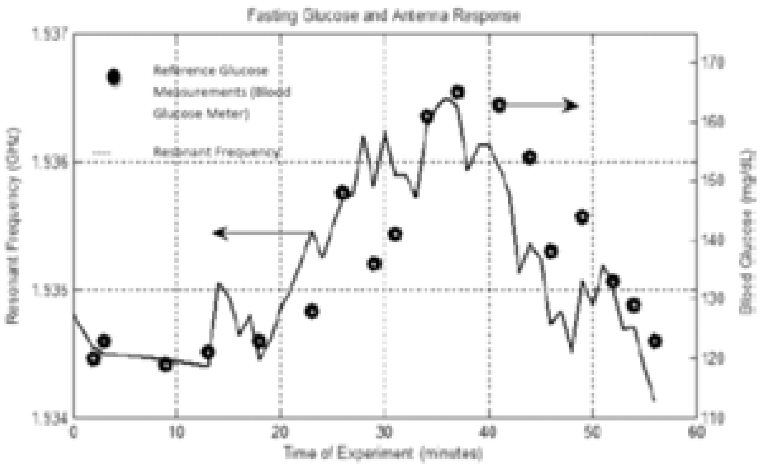

Figure 11. Measured resonant frequency of antenna vs. blood glucose levels.

Tissue Type	Original Blood Model [32]	Modified Blood Model
ε_∞	4	2.8
$\Delta\varepsilon_1$	56	56.5
$\Delta\varepsilon_2$	5200	5500
$\Delta\varepsilon_3$	0	0
$\Delta\varepsilon_4$	0	0
τ_1	8.377e-12	8.377e-12
τ_2	132.629e-9	132.629e-9
τ_3	-	-
τ_4	-	-
α_1	0.1	0.057
α_2	0.1	0.1
α_3	-	-
α_4	-	-
σ	0.7	0.5

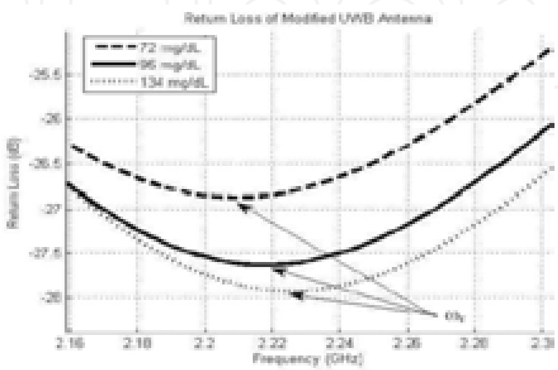

Figure 12. Tissue layers used for simplified human body model and modified UWB antenna return loss for varying glucose concentrations.

Tissue type	Original blood model [32]	Modified blood model
ε_∞	4	2.8
$\Delta\varepsilon_1$	56	56.5
$\Delta\varepsilon_2$	5200	5500
$\Delta\varepsilon_3$	0	0
$\Delta\varepsilon_4$	0	0
τ_1	8.377e−12	8.377e−12
τ_2	132.629e−9	132.629e−9
τ_3	–	–
τ_4	–	–
α_1	0.1	0.057
α_2	0.1	0.1
α_3	–	–
α_4	–	–
σ	0.7	0.5

Table 1. Parameters of original and modified blood Cole-Cole models.

4.5. Analytical model of narrowband antenna

A method to determine a lumped element equivalent circuit has been applied successfully for dipole antennas [22]. This method has been applied to this planar antenna, with some minor additions (**Figure 13**). The feed network can be modeled as a transmission line between the radiator and the port. **Figure 14** shows the real and imaginary impedance of the simulated antenna and the equivalent circuit model. Good agreement can be seen between the model and the simulated data. The values of this model that match the free space resonance at 1.8 GHz can be found in **Table 2**.

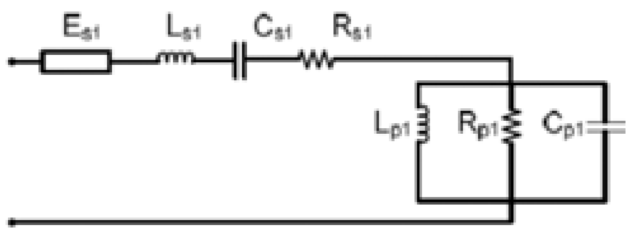

Figure 13. Analytical model accounting for antenna orientation used to validate model.

The presence of tissue near the antenna will act as an additional capacitor C_{p2} present in the parallel resonant RLC network that is a function of the tissue dielectric properties and position (**Figure 15**). The C_{p2} capacitor values have then been determined in the equivalent circuit to match the antenna reactance from the HFSS simulations. The various C_{p2} values determined are plotted in **Figure 16** as a function of the dielectric permittivity and distance from the antenna. It can be seen that for all distances, the changes in C_{p2} are nearly a linear function of permittivity, which would be expected for a capacitor behavior.

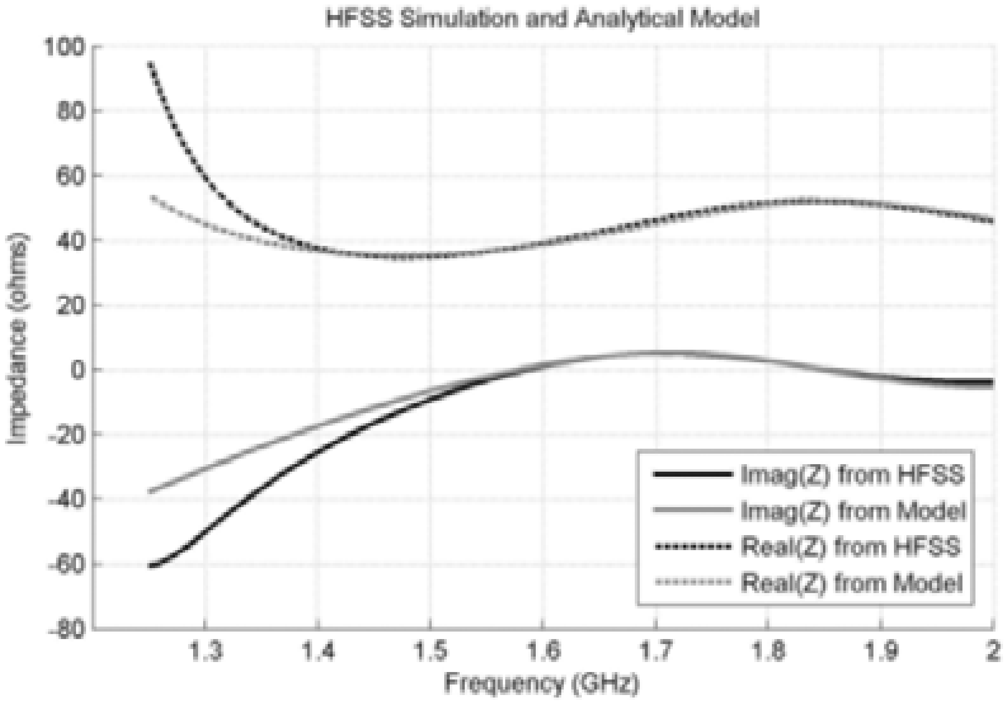

Figure 14. HFSS simulation and analytical model.

E_{S1}	L_{S1} (nH)	C_{s1} (pF)	R_{s1} (Ω)	L_{p1} (nH)	R_{p1} (Ω)	C_{p1} (nF)
50 Ω transition line 230 degree delay at 1.8 GHz	1.5	2.25	29	1.32	36.5	3.5

Table 2. Lumped element values of analytical model.

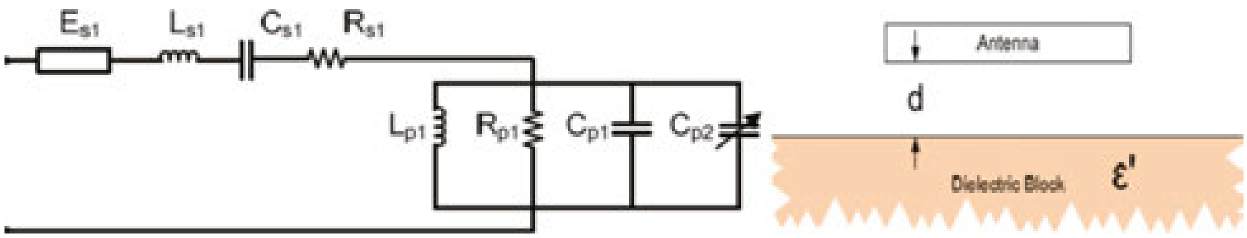

Figure 15. Analytical model accounting for tissue layers and antenna orientation used to validate model.

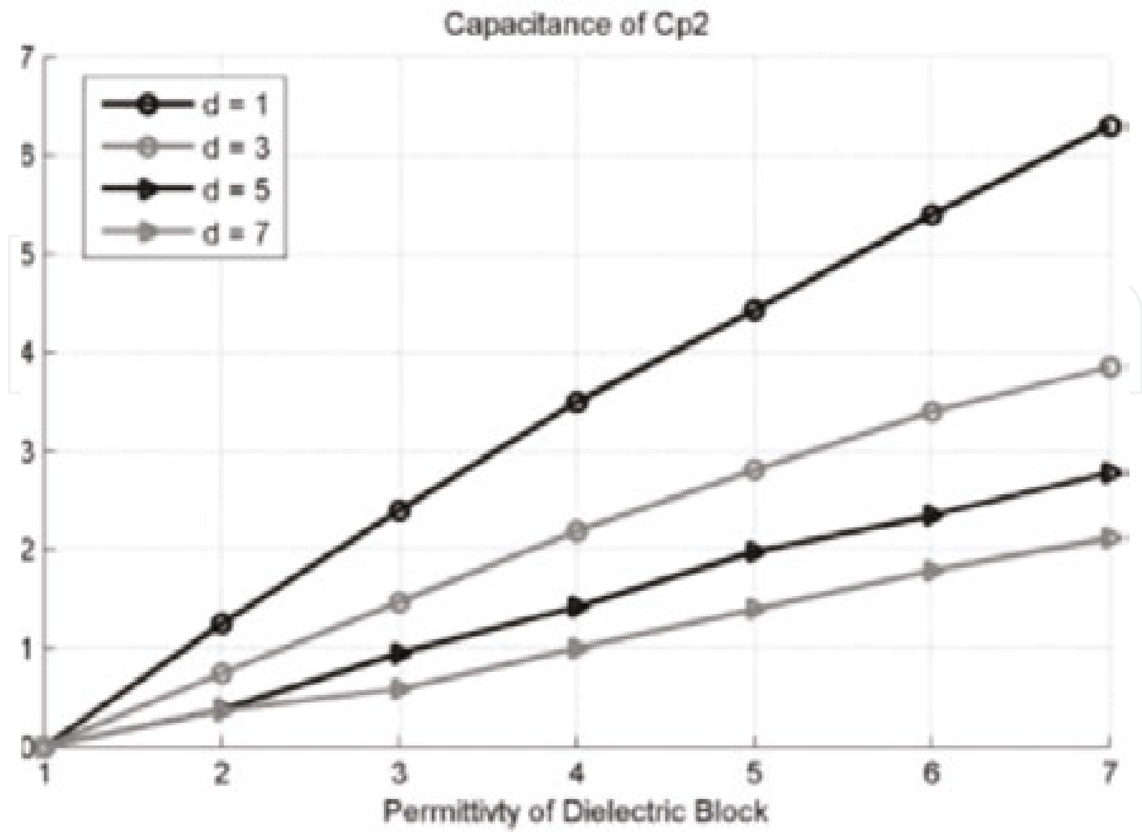

Figure 16. Capacitance of Cp_2 for various dielectrics.

5. Microstrip cavity resonator biosensor (MCRB)

Microwave applications have assumed considerable importance in medicine because they are effective in the reduction on the mental and physical burden borne by patients with non-invasive way. Such applications are of three types [23]:

a. Thermal treatments which use microwave energy as a source of heat. Antennas used to elevate the temperature of cancer tissues are located inside or outside of the patient's body, and the shapes of the antennas used depend on their locations.

b. Diagnosis and information gathering inside the human body (e. g., by computerized tomography and magnetic resonance imaging) and noninvasive temperature measurement inside the human body. Telecommunications illustrates the importance of functions of implantable medical devices which need to transmit diagnostic information.

c. Gathering of medical information on the human body from outside the body (bio-sensors), techniques in this category are considered to be an exertion of communication technologies.

http://dx.doi.org/10.5772/64773

The challenges may be summarized as follows:

1. **Application–driven challenges**

   *Data fusion (aggregate and filter)

   *Support of multiple data rates

   *Robustness, zero maintenance

   *Security and privacy at low energy cost

2. **Technology challenges**

   *Low complexity/low–power designs

   *Smart personal networks and sensors

   *Integration of heterogeneous networks considering BWCS.

Antennas and propagation are the most basic points for integrating wireless body area network (WBANs), wireless sensor network (WSNs), and personal area network (WPANs) into future wireless heterogeneous networks which is a necessary step to shape the 4G landscape. Body–centric communications is a research topic combining WBANs, WSNs, and WPANs. These communication techniques are built basically on biosensors that antenna are acting as the vital component in their structures [23].

An antenna is a structure, usually made from a good conducing material that has been designed to have a shape and size such that it will act as an electromagnetic sensor that radiates/receives power in an efficient manner. It is a well-established fact that time-varying currents will radiate electromagnetic waves. Thus, an antenna is a structure on which time-varying currents can be excited with relatively large amplitude when the antenna is connected to a suitable source, usually by means of a transmission line or waveguide. There is an endless variety of structural shapes that can be used for an antenna. However, from a practical point of view, those structures that are simple and economical to fabricate are the most commonly used. In order to make antenna work adequately efficiently, the minimum size of the antenna must be comparable to wavelength.

5.1. Microstrip patch antenna

Microstrip antenna is one of the most common planar antenna structures used. Extensive research development aimed at exploiting its advantages such as lightweight, low cost, conformal configurations, and compatibility with integrated circuits have been carried out. For many applications, the advantages of microstrip antennas outweigh their limitations. Initially, microstrip antennas found widespread applications in military systems such as missiles, rockets, aircrafts, and satellites. Currently, these antennas are being increasingly used in the commercial sector at different applications due to the reduced cost of the dielectric substrate material and mature fabrication technologies. With continued research and development and increased usage, microstrip antennas are ultimately expected to replace conventional antennas for most applications such as mobile and satellite applications, radar antennas Wi-Fi applications, biomedical application [24–26].

One of the most important requirements in wireless biosensors is the mobility of the device; its size can be reducing with keeping same performance. As shown in **Figure 17**, the simplest configuration of microstrip antenna path is dielectric substrates with metal patch forms one side and ground plane on the other side. Regular patch shapes are always preferred for easy analysis and performance predications. Rectangular and circular patches are the basic shapes that most commonly used in microstrip antennas. Ideally, the dielectric constant ε_r, of the substrate should be low ($\varepsilon_r < 2.5$), to enhance the fringing fields that account for radiation. However, other performance requirements may dictate the use of substrate whose dielectric constant can be greater. As in our prototype blood sensor, the miniaturized size is one of the main challenges; hence, higher dielectric constants are desired ($\varepsilon_r < 10.2$).

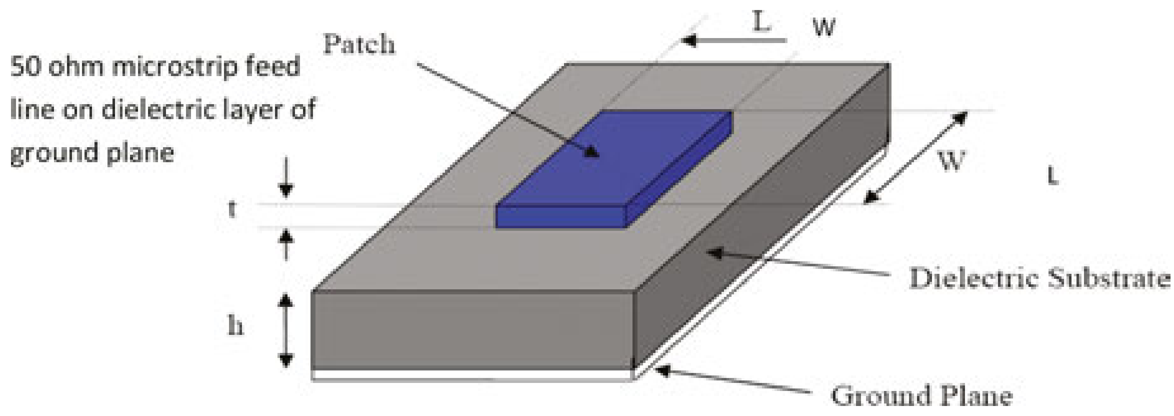

Figure 17. Proximity-coupled feed microstrip patch antenna.

Recently, a big attention is devoted towards compact microstrip antenna design with multi-function as multi-frequency bands, dual polarization, broadband, and high gain. Several open literatures introduce inherent solution for narrow bandwidth of the microstrip antenna as proximity-coupled feed, capacitive-coupled feed, and 3D transmission line feed.

In our prototype system, proximity-coupled feed antenna is used as shown in **Figure 17** to ensure continuous clear surface of the antenna patch metal; hence, it acts as the blood sample holder [25].

One of the most famous blood diagnosis methods is the surface plasmon resonance (SPR) in thin metal layers. It is one of the most sensitive label-free methods for the measurement of the reaction dynamic of biological molecules on gold surfaces. The application of modern powerful CCD cameras provides the possibility of SPR Imaging. In this case, the incident laser light is fixed at an angle which is slightly shifted away from the minimum of the SPR resonance curve to the middle of one wing. Variations of the intensity of the reflected laser light are proportional to the shift of the resonance minimum caused by surface reactions. This enables simultaneous monitoring of many reactions at identical conditions. However, providing high throughput, the imaging methods usually possess a degraded detection power compared with single-spot measurements wireless communication that can be used. The cost and time consuming of such systems create the need of other fact, cheap, and mobile diagnostic systems.

5.2. Resonator biosensor

A typical application of the field of biosensors is the detection of biological substances by measuring changes in electrical properties of the materials. Biosensors are now being employed in medicine, biotechnology, and environmental monitoring. The use of biosensor for rapid detection of the enteroviruses will limit the need for sophisticated laboratory diagnostic methods that needs long time and expert scientists to perform the test. Usually, it takes at least 12 h of laboratory work to make sure that a clinical sample is safe. The physician in the field normally do fast and simple tests like physical examination of the clinical sample, performing some preliminary tests, and then gives a fast decision regarded as potentially safe or not.

All these tools are available today; however, until now there exists no fast and sensitive method to know whether the clinical sample is infected with enteroviruses or not. Thus, the risk is still very high that the physician comes to a wrong decision on the health status of the clinical tested sample. If the clinical sample is infected, it means that there is a great possibility for the enteroviruses outbreaks which initiates danger risk.

Nowadays used methods for diagnostic screening have reached a high degree of accuracy, sensitivity, and reliability. Most methods achieve an accuracy of more than 99.9%. The drawback of these methods is that they are time consuming. The accuracy is mainly based on very complicated enzymatic activity (ELISA) or radioimmunoassay (RIA) or nucleic acid-based reactions (PCR, hybridization) that lead to visual changes that can be measured. The accuracy of these biological methods depends on highly sophisticated reactions that need to be done in well-equipped laboratories with well-trained personnel. Within the project, a fast and sensitive testing method for biological sample will be developed. This method has the potential to detect the existence of pathogens. The transducer principle is based on microwave cavities resonator biosensor (MCRB), which is known to be a sensitive label-free method that allows detecting receptor-legend binding. Using homogenous distributed spots allows reaching high accuracy compared to the state of the art. Therefore, we meet the request for "*new screening techniques*," which are "*sensitive enough to avoid false negatives*." The **MCRB** system is also capable to detect multiple pathogens simultaneously if antibodies of all these pathogens are immobilized on the transducer chips. Only true/false indicator will be detected. **Figure 18** shows some of our antenna simulation results of reflected scattering parameters change due to the immobilization of sample layer upon the microstrip antenna surface. **Figure 18** illustrates that there is a detectable shift in resonating frequency and reflection coefficient due to the change in the tested sample characteristics, hence verifying the proposed research idea, that depends on measuring this change due to the presence of enterovirus infection in the tested sample as will be described later in next section. This allows a very rapid testing for pathogens in one single procedure. Thus, this method is fast and cheap, and therefore, meets the requirements for "*development of more cost-effective approaches*." The developed system will finally by clinically show its abilities in detecting pathogens in any biological sample. To be able to carry out statistically relevant tests, numerous test runs will be necessary per pathogen [26, 27].

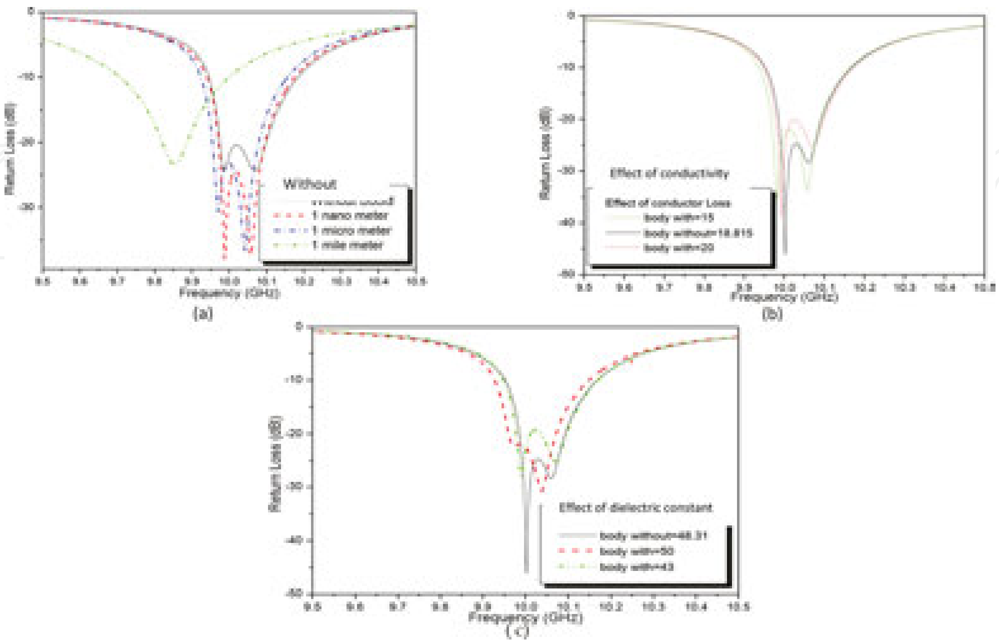

Figure 18. Simulation results of proximity-coupling microstrip antenna reflection coefficients with changing characteristics of sample deposited layer on antenna surface. Effect of changing (a) layer thickness, (b) layer conductor loss, and (c) layer dielectric constant.

The effect of sample characteristics is shown in **Figure 18** that shows in part (a) the effect of deposited sample layer thickness on antenna reflection coefficient. Part (b) shows the effect of sample layer deposition on the measured conductor loss, while part (c) shows same effect on changing the dielectric constant. These simulations are done using electromagnetic readymade software package of (high-frequency structure simulation, HFSS) for proximity coupling fed microstrip antenna at operating frequency of 10 GHz. The results of **Figure 18** verify our proposed idea of MCRB. Many studies have been devoted to the absorption of proteins onto solid surfaces and the immunological reaction between antibody and antigen.

The proposing of a micro-immunosensing diagnostic assay is based on the very specific immune reaction between antigen and antibody. The assay can be manufactured by first absorbing a layer of antibodies that has multiple specificities to enteroviruses and then immobilized on an-active gold-coated dielectric slide (low-profile microstrip antenna surface), which forms one wall of a thin flow-cell, while the other interacting in an aqueous buffer solution that is induced to flow across this surface.

When the biological sample, containing the antigen the antibodies are directed, is brought in contact with the coated solid phase, the specific immune reaction occurs and the marker antigen will bind to the antibody. This binding, resulting in a layer growth that can be detected, for example, when electromagnetic wave is incident on the antenna surface coated with gold, reflection coefficient S_{11}, and input impedance (real and imaginary) can be measured by (vector network analyzers) VNA. The reflection coefficient amplitude in dB, input impedance in ohms, and frequency resonance value in GHz are expected to be changed from case of normal clinical sample layer to infected clinical sample layer or to infected sample layer with antigen/antibodies embedded. Recording this change and classifying it, after reading of large number of samples, one can detect in fast way the infection of enteroviruses in clinical sample. Software code is developed for automatic reading, classifying, and determining the sample infection afterwards. This procedure depends on small miniaturized size of microstirp antenna to act as sample plate. Coating the antenna surface with gold will be used to isolate its surface from outside environment and exclude any unwanted surrounding parameters that may effect on the accuracy or sensitivity of readings. Proper thickness of sample layer deposited on antenna surface would be determined through simulations first and then through pre-experimental tests. The expected frequency range of operation will be in C-band (2–3 GHz), Bluetooth, and ISM band (industrial, scientific, and medical) and/or in X band (from 8 to 12 GHz). This will be decided according to the system sub-components purchase availability in local market or abroad [28].

Also, the system size allows for mobile applications. No need for connection to host computer as in SPR system. The whole test will be done in the field with no need to return or connect to the laboratory since a comparison with the calibration levels will be done automatically through the developed control software. The other advantages are the low cost of electromagnetic system and the reduced hazardous effects than other sources as lasers, IR, etc.

First, clean sample layer will be deposited with normal buffer electrical properties. The output signal level and frequency will be measured accurately to determine the standard references.

Second, the same measurements will be done for the samples collected from tested area layered onto the chip; various samples showing different stages of different titer of viruses will be used to standardize the test. The antenna chip prototype is as shown in **Figure 19**. It consists of a planner antenna with metal surface, coated with gold (to prevent oxidation), a measuring facility for power level and frequency, electromagnetic source, mechanical micro-pump, etc. The whole system hardware block diagram is as shown in **Figure 20**. Third, a thin-film sample under test will be deposited on the surface with micro-fluid injection procedure.

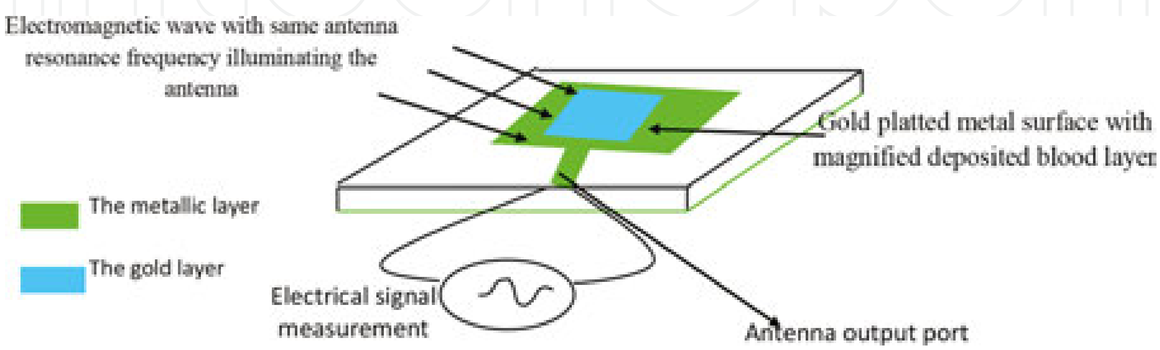

Figure 19. Microwave cavity resonator bio-electromagnetic sensor system verification idea.

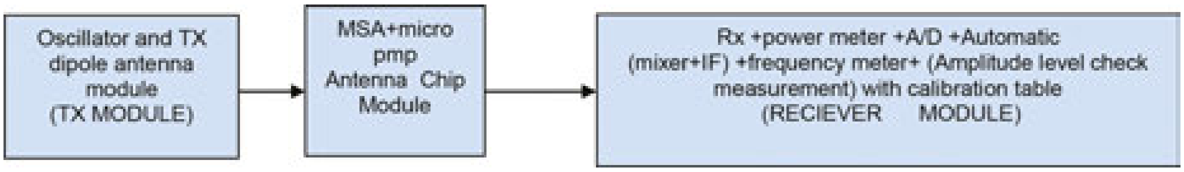

Figure 20. Block diagram of mobile virus diagnosis system.

The output signal level which depends on the electrical properties of the deposited layer will be measured accurately. Comparison with calibration table will be done automatically. From the signal level reading, a decision of infection existence will be automatically taken. The knowledge of the used antigen gives information about viruses that need to be detected. The frequency of operation is in the range of 2–3 GHz in C-band and/or 8–12 GHz in X-band; so the antenna chip size will be in the range of few square mms. The novelty in this idea, as mentioned earlier, is the measurement of the change of the electrical properties which makes the idea free from the molecular size limitation that exists in other systems as optical biosensors. Same idea but with different experimental procedures, as microwave waveguide resonator or microwave probe insertion, is verified in the literature [24–29].

Improving the screening tests in terms of speed and costs for biological samples will cut the costs and will thus give a direct economic value. Better screening methods decrease the risk of infection, and most importantly will provide a perfect tool to screen more enteroviruses. Nowadays, screenings include a limited number of pathogens due to cost and/or scientific reasons. The conceived system consists mainly of (MCRB) cavity resonator chips. The instrument is primarily designed for detecting multiple pathogens in sample. Due to the limited resources of this project, we concentrate on the relevant enteroviruses. Otherwise, the need of resources for performing relevant tests would by far exceed the budget. But it has to be emphasized that this system has the potential to detect more than one pathogen, simultaneously if the corresponding receptors are immobilized on the transducer chip [29].

The MCRB system could become a standard system for screening donor blood. Depending on the application, the system can be designed for different levels of complexity. The result of the screening can give quantitative figures for each pathogen. The high specificity, accuracy, and sensitivity of the new method help to reach the goal of avoiding false positives as well as false negatives. Despite the accuracy of the method, it is very rapid and can give results in few minutes. This ability together with the potential to screen for numerous pathogens makes the MCRB system well suited for screening donors prior to organ transplantations.

A low-profile microstrip disc antenna with micorstrip line proximity coupling feed is proposed in order to keep the antenna surface clean for imposing the blood sample layer. The patch is placed alongside a small rectangular ground plane co-planar to it as shown in **Figure 21a**. Antenna prototype is designed to operate at 2.4 GHz. **Figure 21** illustrates the fabricated antenna. The resonating antenna with deposited layer of normal blood serum is considered the reference of the measurements from which the changes due to the viral layer deposition are measured. The Agilent E8719A vector network analyzer is used for preliminary prototype measurements. This is replaced by portable transceiver Ettus N210 with open source control software in the final prototype design.

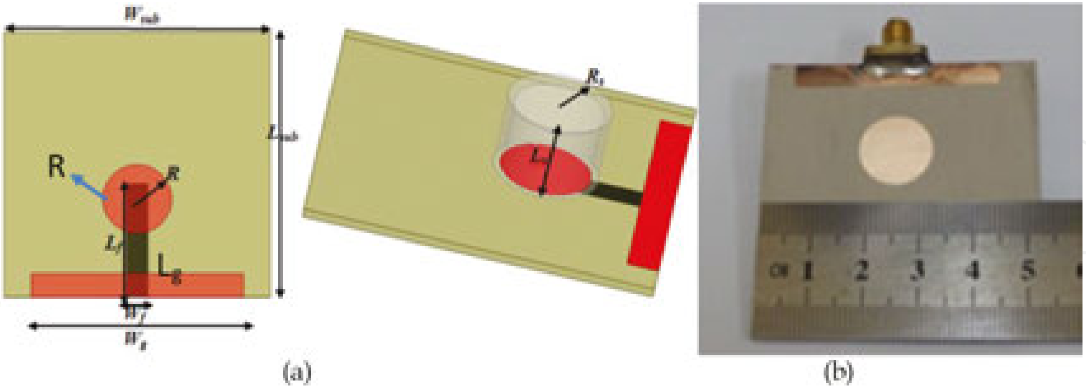

Figure 21. (a) Geometry antenna configuration and (b) proposed microstrip antenna with gold platted surface.

Figure 22 illustrates the results for different concentrations of attenuated G1P(8) Rota virus. The scattering parameter $|S_{11}|$ for antenna in installation steps of the chamber/housing over antenna shifts the resonating frequency down to 1.88 GHz with $|S_{11}| = -15$ dB as in **Figure 22a**. This can be attributed due to resistive loading effects of glass chamber and rubber gasket. Starting viral immobilization on the sensor surface shifts the cavity resonating frequency down to 1.865 GHz with $|S_{11}|$ equal to −13 dB at the fourth viral concentration of 1×10^6 virus particles. These preliminary results verify the sensor idea practically; however, more investigations are still running.

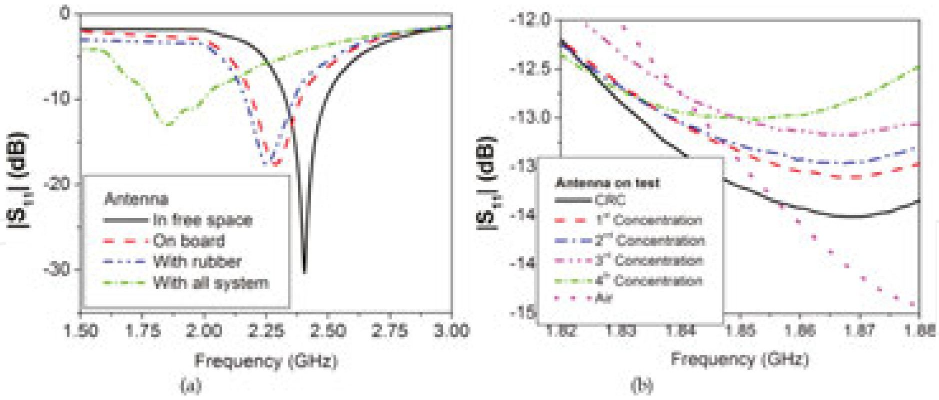

Figure 22. Measurements of reflection coefficients $|S_{11}|$ at 2.4 GHz of micro-immunosensor for different installation steps in part (a) and for different viral concentrations in part (b).

The antenna was simulated using 3D full-wave electromagnetic simulator, high-frequency structure simulator (HFSS) version 13. The dielectric constant change was measured using blank buffer solution used to dilute Rota virus stock solution using DAK (dielectric assistive kit). The system measures liquids, solids, and semi-solids dielectric constant over a broad range of frequency from 10 MHz to 20 GHz. The measurement method is fast and nondestructive for the material under test. **Figure 23** shows the changes due to different concentrations of Polio virus.

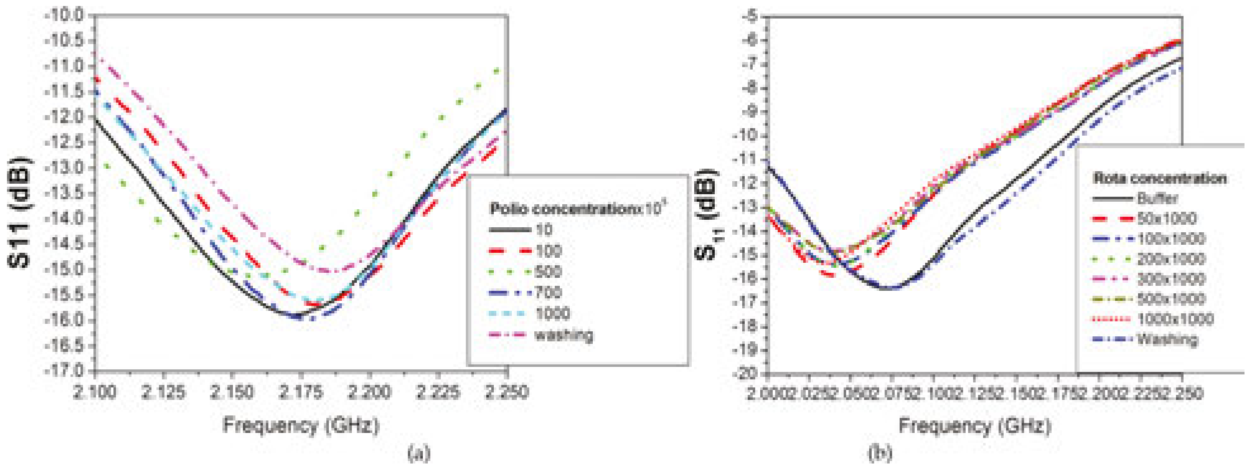

Figure 23. The effect of type A antenna S_{11} change due to insertion of different virus concentrations: (a) Polio and (b) Rota.

6. Ground penetrating radar (GPR)

For searching on underground mummies or any biological bodies as well as water the ground penetrating radar (GPR) is used. GPR is a nondestructive technique. To enhance the performance parameters of the GPR antennas, different parameters should be considered. As mentioned earlier, when the transmitting and/or the receiving antennas are placed close to the ground, they suffer from significant changes in their input impedance. This change is a function of the antenna elevation angle and the soil type. Different techniques have been proposed to maintain the input impedance matching conditions. It has been shown in [30] that the input impedance of a bow-tie antenna changes with the flare angle variation, giving the possibility of adaptive antenna matching. In bowtie antenna, the input impedance is affected by the ground plane; however, one can modify it by adjusting the design flare angle to keep the reflections in the minimum level at the antenna terminals.

Other techniques have also been reported regarding the implementation of impedance matching networks for different antenna systems to achieve maximum matching condition, such as, radio frequency-microelectromechanical systems (RF-MEMS)-based matching module for adaptive antennas where RF-MEMS devices are used for the implementation of variable capacitors at the antenna input for better transfer of power to the antenna, or the use of a pi-network matching circuit adaptively controls by two varactors, reducing the refection between the matching circuit and the RF front end of a transceiver.

Another critical parameter for the GPR antenna system is system directivity. High directive antennas for GPR systems are needed to avoid the loss of power. Recently, several antennas

http://dx.doi.org/10.5772/64773

have been reported where the use of electromagnetic bandgap (EBG) and frequency selective surface (FSS) shows highly directional radiation properties. Another technique to increase the antenna system directivity is to use an antenna array rather than one single radiating element. To keep the system low profile, planar antennas are recommended for such application. On the other hand, mutual coupling between the different radiating elements might take place. Some structures have been proposed to reduce the mutual coupling between the radiating elements of microstrip antenna arrays such as cavity backed and substrate removal microstrip antennas. The other approach is using metamaterials insulator between the antenna arrays elements to reduce the mutual coupling. These metamaterials are designed to operate at certain frequency band gap or insulating region where the effective permittivity and permeability have opposite signs. However, this insulating/band gap frequency range is usually narrow bandwidth which resembles the main limitation with this approach.

GPR technique uses transmitting and receiving antennas separated by a small fixed distance, to send electromagnetic (EM) energy into the ground and then record the returning signals. Depending on the application, different antennas are used where low-frequency antennas provide greater penetration, but lower resolution and high-frequency antennas have limited penetration but higher resolution as shown in **Figure 24**.

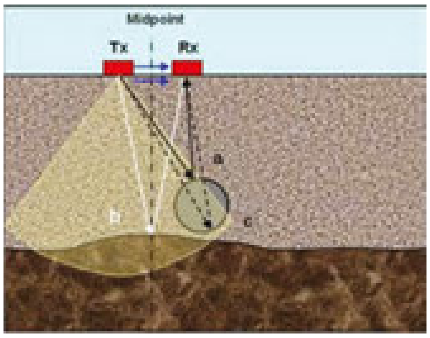

Figure 24. EM wave sent into the ground by TX antenna and the reflected EM wave received by RX antenna received wave discontinuity should be at the top and bottom of a buried object.

As mentioned earlier, ground penetrating radar consists of a transmitting antenna which is used to transmit a signal to the ground. Depending on the received signal scattered from the buried body in the ground, identification of the underground target may take place. This is based on the fact that the velocity of propagation of electromagnetic (EM) waves, given by v (m/s), depends on the complex dielectric permittivity of the medium of propagation, where the complex dielectric permittivity of the medium is given by $\varepsilon^*(f) = \varepsilon'(f) - j\varepsilon''(f)$. It should be noted that the imaginary part of the complex dielectric permittivity $\varepsilon''(f)$ expresses the energy dissipated in the medium, while the real part $\varepsilon'(f)$ is associated with the capability to store energy when an alternating electric field is applied.

An important parameter that should be considered in GPR operation is that the complex dielectric permittivity of the soil under test varies considerably with the frequency of the applied electromagnetic signal. This frequency dependence of permittivity is a function of the polarization arising from the orientation with the imposed electric field of molecules that have permanent dipole moments. The mathematical formulation of Debye describes this process for pure polar material by [31]:

$$\varepsilon^*\left(f\right) = \varepsilon_\infty + \frac{\varepsilon_s - \varepsilon_\infty}{1 + \left(\frac{jf}{f_{rel}}\right)} - \frac{j\sigma_{dc}}{2\pi f \varepsilon_o} \tag{13}$$

where ε_∞ represents the permittivity at frequencies so high that molecular orientation does not have time to contribute to the polarization, ε_s represents the static permittivity (i.e., the value at zero frequency) and f_{rel} (Hz) is the relaxation frequency, defined at which the permittivity equals $(\varepsilon_s + \varepsilon_\infty)/2$. The separation of Eq. (13) into real and imaginary parts is shown in **Figure 25**, for a material of $\varepsilon_s = 20$, $\varepsilon_\infty = 15$ and $f_{rel} = 10^{8.47}$ Hz (300 MHz). **Figure 25** shows the real part and imaginary part values analyzed by Debye model. From the figure, the permittivity has constant values with zero losses at low and high frequencies, while losses appear at intermediate frequency.

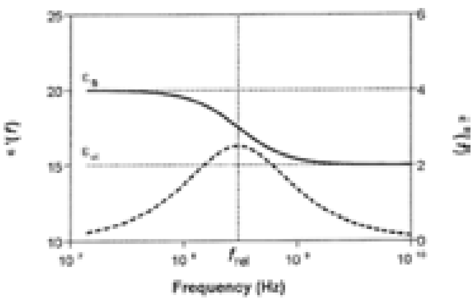

Figure 25. Example of the Debye model for the real part (solid line) and imaginary part (dashed line) of the permittivity.

The Debye parameters of water are $\varepsilon_s = 80.1$, $\varepsilon_\infty = 4.2$, and $f_{rel} = 10^{10.2}$ Hz (17.1 GHz) at 25°C. In sandy soils, most water is effectively in its free liquid state. In the case of GPR measurements, $\varepsilon''(f)$ is often small compared with $\varepsilon'(f)$. The real part of the permittivity of water within the megahertz to gigahertz bandwidth is given by **Table 3**:

Temperature (°K)	279	297	303	337
Relative dielectric	86	79	75	66

Table 3. Dielectric permittivity measurement of drinkable water [18].

For reliable measurements, the multi-offset reflection method will be used where multiple measurements with different antennas separations (radar transmitting and receiving antennas) are performed. More precisely, the wide angle reflection and refraction (WARR) configuration will be adopted in the design architecture and measurement setup [32]. As shown in

Figure 26 (a), the WARR setup consists of a transmitting antenna at a fixed location, while the distance between the receiving antennas is increased stepwise.

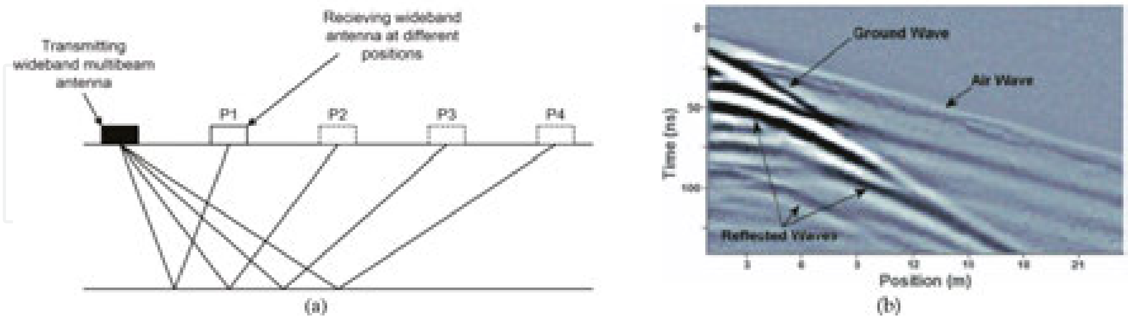

Figure 26. (a) Wide angle reflection and refraction (WARR) acquisition, (b) common-midpoint (CMP) measurement made with a 100 MHz antenna at the Cambridge Research Station, University of Guelph, ON, Canada.

To collect the reflected data, only one antenna will be used. This antenna will be displaced continuously along the survey line with a fine spatial interval between two receiving positions and continuous-wave radar (CW) modulation scheme will be adopted. Continuous bottom layers with different soil water content or more generally with sufficient permittivity contrast can be easily identified as this result in consistent reflected waves data that can fit the following condition (see illustrative examples of **Figure 26 (b)**)

$$v_{soil} = \frac{2\sqrt{d^2 + 0.5a^2}}{t_{rw(a)}} \tag{14}$$

where $t_{rw(x)}$ is the zero time corrected arrival times of the reflected waves, a is the antenna separations, d is the depth of the reflecting layer, and v_{soil} is the root mean square (RMS) velocity down to the bottom of that layer. The RMS velocity and the depth d can be calculated by solving Eq. (14) for different antenna separations [33]. Naturally, the soil beneath the surface till the water level (within the penetration range allowed by the GPR) consists of multiple horizontal layers (reflectors). Eq. (15) is used together with the Dix formula [34] in order to estimate the dielectric constant of each layer as formulated by Eq. (16).

$$v_{\int,n} = \sqrt{\frac{t_{rw,n}v_{soil,n}^2 - t_{rw,n-1}v_{soil,n-1}^2}{t_{rw,n} - t_{rw,n-1}}} \tag{15}$$

where $v_{soil,n}$ and $v_{soil,n-1}$ are the average interval velocities from the surface down to the bottom of layers n and $n-1$, respectively. $t_{rw,n}$ and $t_{rw,n-1}$ are the two-way travel time down to the bottom of layers n and n−1, respectively, the upper layer of the soil being denoted by $n = 1$. The thickness of layer n is thus given by Eq. (16) as follows:

$$d = \frac{v_{i,n}\left(t_{rw,n} - t_{rw,n-1}\right)}{2} \tag{16}$$

Upon determining the velocity profiles with the depths of the corresponding layers, the corresponding permittivity profile curves can be extracted using the relationship between the interval velocity v_i and the dielectric constant. The imaginary part of the water permittivity becomes negligible with respect to the real part and the former relationship simplifies to the following:

$$v(f) = \frac{c}{\sqrt{\varepsilon'}} \tag{17}$$

Upon determining the measured water permittivity, water content-permittivity relationships can be used to estimate the volumetric water content. Different relationships can be then used as reported in [33–36].

6.1. Quasi-Yagi antenna with size reduction for water detection

Figure 27 shows the geometric structure of planar Yagi-uda antenna printed on commercial FR4 substrate with thickness of 9.5 mm. The antenna shape consists of T-shaped dipole driver and two parasitic meander shapes. The feeding system is printed on the bottom layer of the substrate with length L_f and S_D. The circular resonator is used to match the input impedance of the antenna to a 50 Ω feeding line. The dimension of the substrate width and the length is 72 × 70 cm^2. A $\lambda/4$ slot line ended with a circular slot of diameter L_D is used for matching the antenna [37, 38].

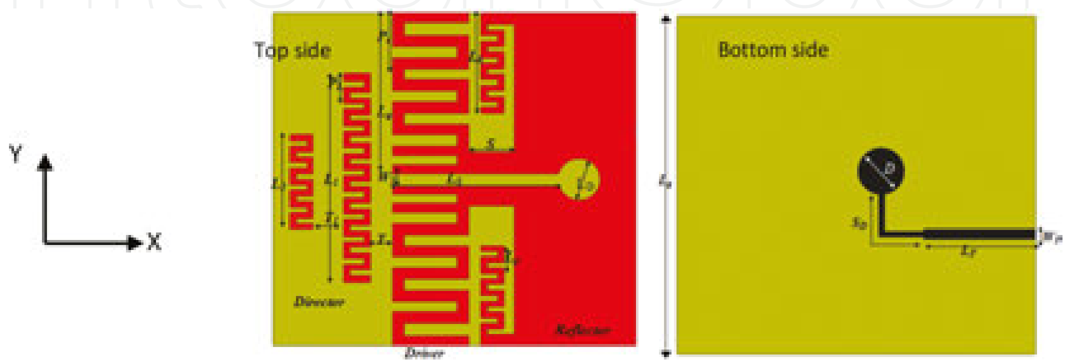

Figure 27. The quasi-Yagi antenna configuration.

Figure 28 shows the Yagi antenna reflection coefficient at frequency range from 50 to 150 MHz with negligible change in the bandwidth due to coupling effect between the antenna driver and director. The coupling effect can be controlled by adjusting the distance between driver and director. **Figure 29** illustrates the reflection coefficient as a function of the balun diameter and its distance from the feeding.

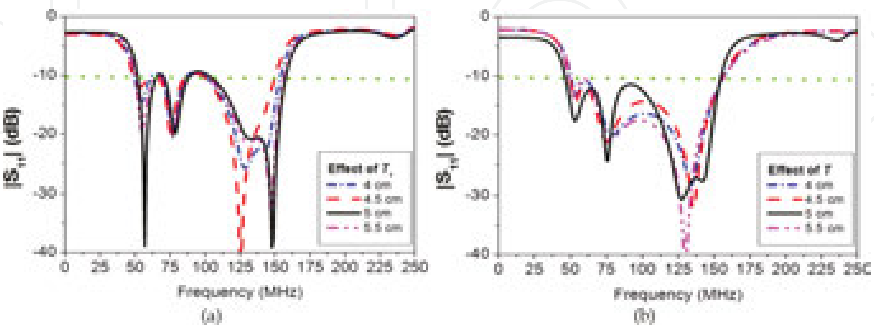

Figure 28. Effect of the length (a) T_1 and (b) Ton the simulated reflection coefficient.

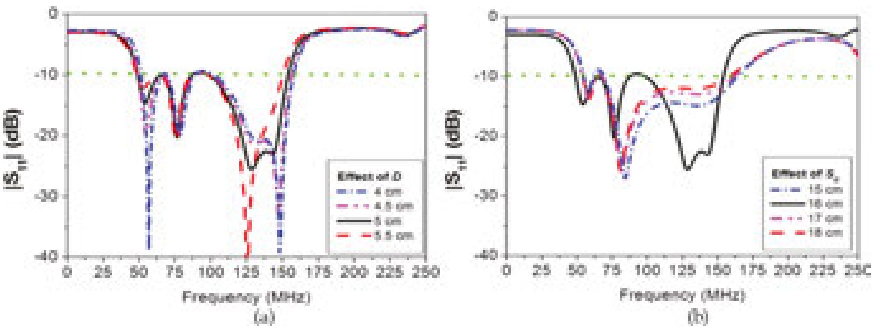

Figure 29. Effect of the length (a) D and (b) S_D on the simulated reflection coefficient.

6.1.1. Ground penetrating radar antenna system

Ground penetrating radar system is used for underground water detection. The operating frequency band extends from 50 to 150 MHz for frequency-modulated continuous-wave (FMCW) radar. The electrical properties of the sand and fresh water layers are investigated using laboratory measurement and EM simulation. The simulated parameters are obtained from Debye dispersive model in the high-frequency structure simulator (HFSS). The radar system as shown in **Figure 30 (a)** requires a high antenna gain to achieve an acceptable scanning resolution. **Figure 30b** illustrates the values of scattering parameters S11 due to projection on the ground surface where the distance between the radiating surface and the ground changes from 0 to 100 cm. The sand layer volume is 300 × 200 × 200 cm^3 as shown in **Figure 30a**. The proposed antenna performance is investigated with and without sand layer as shown in **Figure 30**. The sufficient distance that keeps the antenna reflection coefficient near from free space is almost about 50 cm as shown in **Figure 31a**.

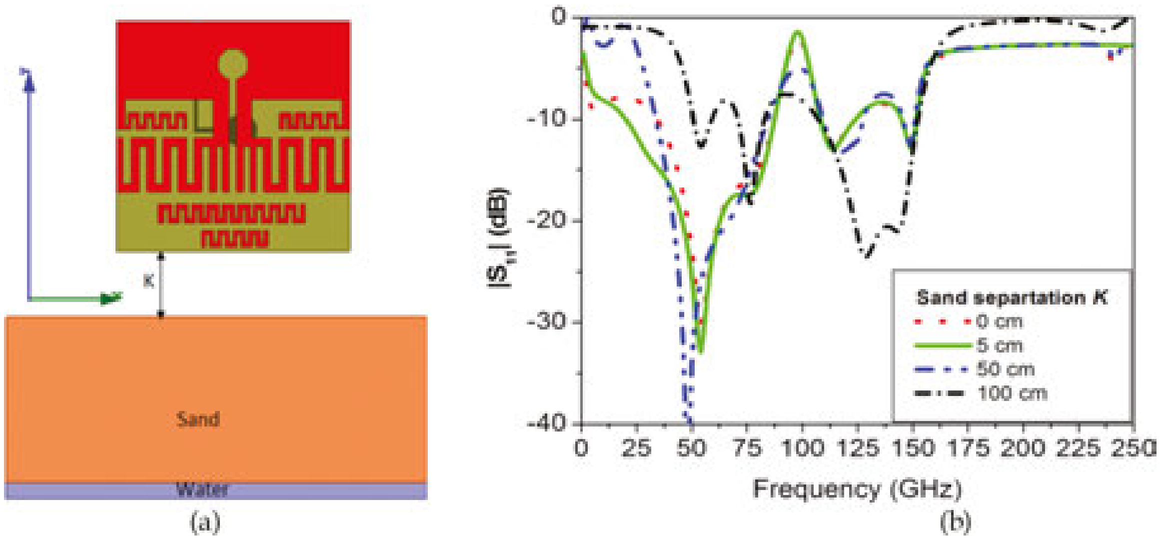

Figure 30. (a) The GPR antenna system for water detection and (b) the effect of K on proposed antenna reflection coefficient.

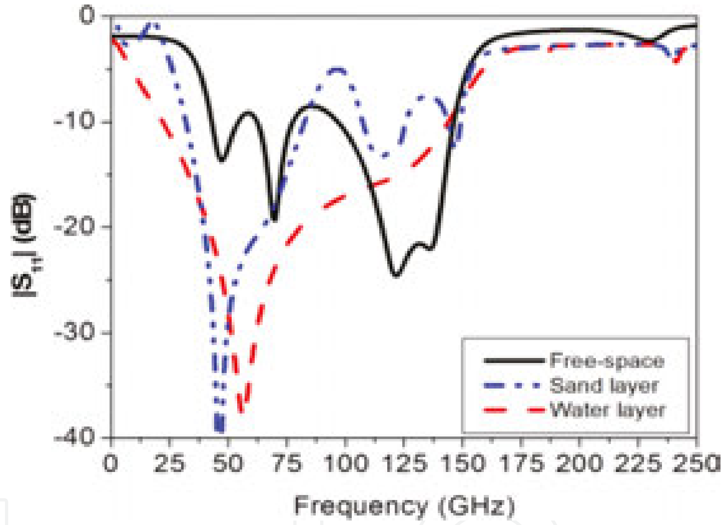

Figure 31. $|S_{11}|$ of the receiver antenna in different cases at K = 50 cm.

6.1.2. Measured results and discussion

The antenna was fabricated as shown in **Figure 32a** using a standard photolithographic etching technology on FR4 substrate with a 100 micrometers copper thickness. **Figure 32b** shows the comparison of the $|S_{11}|$ between measured and simulated results of the optimized antenna which are in fairly good agreement. The antenna measured bandwidth is from 56 to 140 MHz for −6dB threshold in reflection coefficient which covers the required application requirements. The slight difference between the measured and simulated reflection coefficient could be attributed to a misalignment between curved microstrip-line and the circular slot of the balun and effect of the SMA connector.

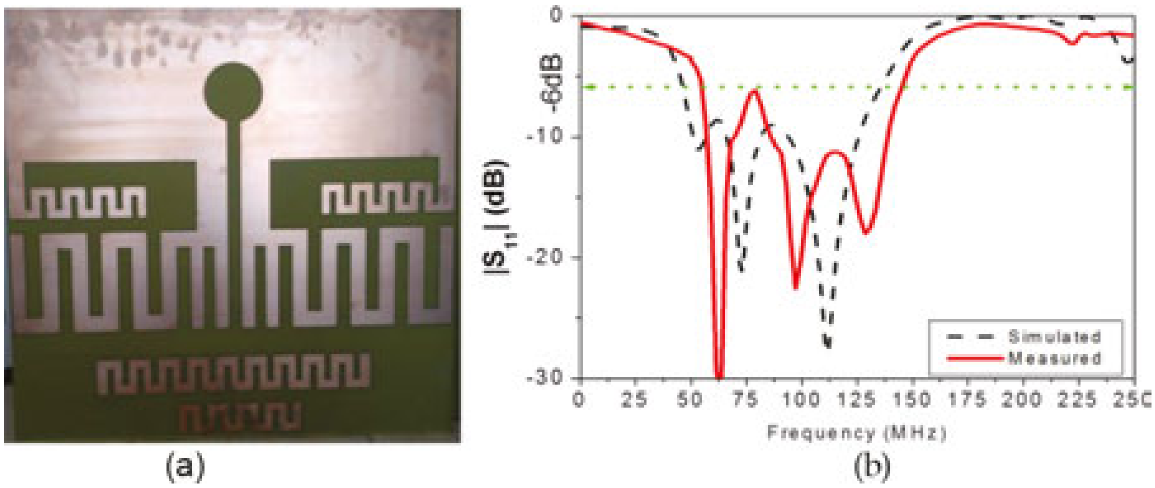

Figure 32. $|S_{11}|$ comparison between measured and simulated reflection coefficient of the proposed antenna.

6.2. Miniaturized log-periodic dipole antenna

The printed log-periodic dipole antenna has many advantages such as lightweight, low costs, and simple to manufacture. **Figure 33** shows the miniaturized printed log periodic antenna (PLPA) which is first order fractal shape. This approach decreases the antenna size with approximately no effect on its bandwidth performance. The proposed antenna printed on thin commercial substrate FR4, 1.6 mm thickness with dielectric constant 4.7 and loss tangent 0.02. The proposed antenna dimensions are shown in **Table 4**. There are seven pairs of array element with scaling factor Ω equal to 0.75 and spacing factor Ψ equal to 0.6. **Figure 34** shows the reflection coefficient response for both conventional, modified LPDA, and FLPDA. The optimized full antenna dimensions are shown in **Table 4**.

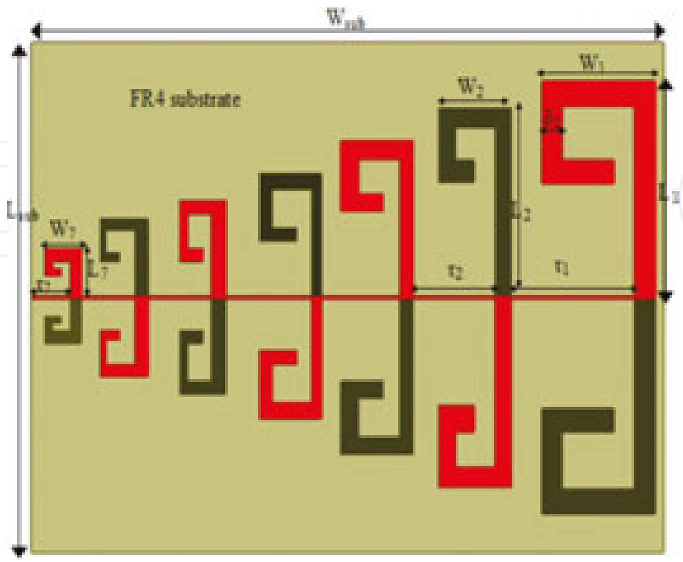

Figure 33. Proposed GPR antenna with first fractal geometry.

L_{SUB}	W_{SUB}	L_1	L_2	L_7	W_F
110	75	32	23.2	7.2	0.32
W_1	W_2	W_7	τ_1	τ_2	τ_7
19.8	12.7	6.5	21.2	14.2	6.8

Table 4. The antenna dimensions in (cm).

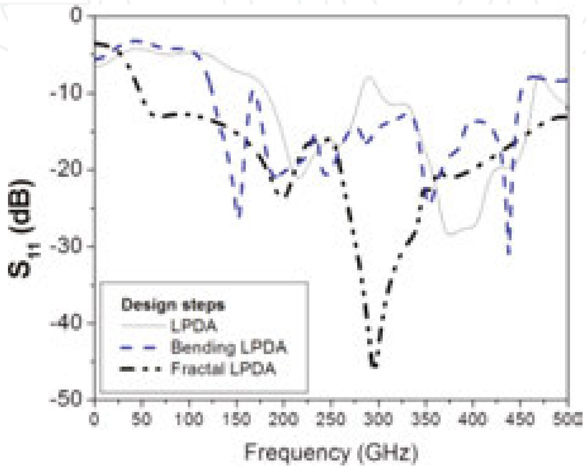

Figure 34. The $|S_{11}|$ design procedures of the proposed antenna.

6.2.1. Ground penetrating radar antenna system

Usually, GPR antennas are placed either on the ground or in a location near the ground with respect to the operating wavelength; hence, each single antenna must satisfy the requirements of radiation and coupling effects. The electrical properties of the sand and fresh water layers are investigated using laboratory measurement and EM simulator. The measurement is done using DAK (coaxial sensor probe and R&S®ZVA vector network analyzers (10 MHz–14 GHz), while the simulated parameters are obtained using Debye dispersive model in the high-frequency structure simulator (HFSS). Both results are very quiet similar as shown in **Figure 35(a, b)**. Debye model is a lossy dielectric dispersive model with a lower frequency near DC, use the loss model material input dialog box to specify the material's conductivity at DC or, its HFSS simulator which has a material specify box in which the conductivity and loss tangent of the material should be defined at DC and low frequency, respectively.

$$\varepsilon_{r_{complex}} = \varepsilon_{r_{optical}} + \left(\frac{\varepsilon_{r_{static}} - \varepsilon_{r_{optical}}}{1 + j\omega\tau} \right) \tag{18}$$

where τ = the relaxation time, $\varepsilon_{rstatic}$ = the static permittivity, and $\varepsilon_{roptical}$ = the high-frequency/optical permittivity. Debye's model is valid for most microwave applications.

http://dx.doi.org/10.5772/64773

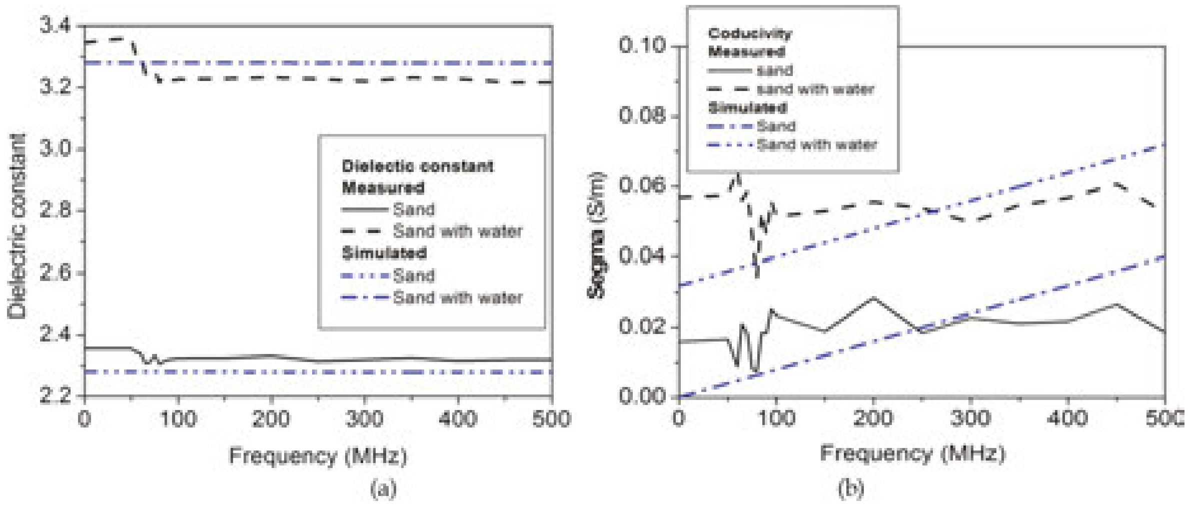

Figure 35. Comparison between measured and simulated electrical properties of sand and sand with water.

In radar system, SAR techniques require high antenna gain to achieve acceptable measurement resolutions. This necessitates that a sufficient large aperture at the lowest frequency to be transmitted. **Figure 36** shows the effect of antenna height on the ground surface (S). It is clear that as distance *S* increases, the reflection coefficient becomes closer to the case of free space. The ground volume is 300 × 200 × 200 cm^3, and it can be seen that the width of the 3-dB footprint increases considerably as the source is raised from the ground.

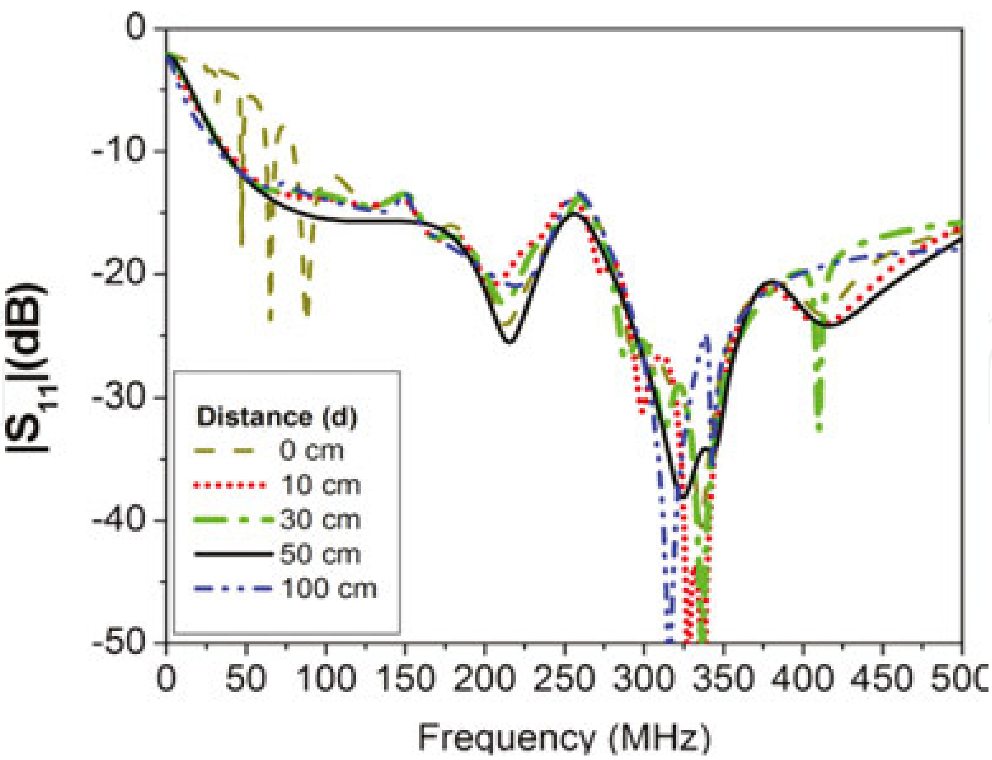

Figure 36. The effect of S on proposed antenna reflection coefficient.

To determine the sufficient distance between both antennas, Snell's law is applied as shown in **Figure 37a**

$$\theta i = \theta r \tag{19}$$

$$tan\theta i \approx \frac{S/2}{q + H} \tag{20}$$

where θi and θr are the incident and reflected angles.

The proposed antenna performance is investigated with and without sand layer. It shows that the antenna directivity is highly increased by about 2dBi as shown in **Table 5**. However, the resonant frequency reduced by about 5% as shown in **Figure 37c**.

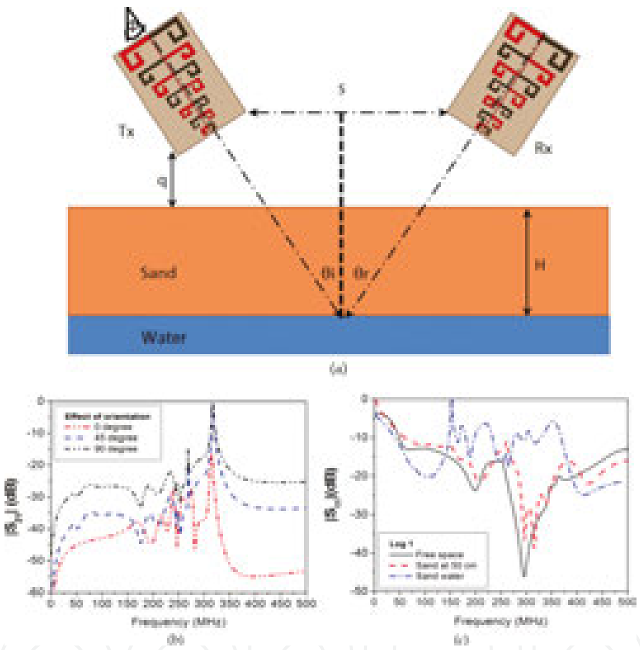

Figure 37. (a) The GPR system for water detection, (b) the $|S_{21}|$ mutual coupling between Tx and Rx, and (c) the receiver antenna in different cases.

Freq (MHz)	Free space	Sand layer	Sand and water layer
Average efficiency%	87	88	86
Average direction (dBi)	3	5	4.8
Average BW (%)	440	400	150
Average beamwidth (degrees)	150	100	100
Average (F/B) (ratio)	1.5	2	1.95

Table 5. The antenna parameters.

6.2.2. Experimental results and discussion

To verify the simulated results, the proposed fractal log-periodic dipole antenna was fabricated using photolithographic techniques and measured using m network analyzer. **Figure 38 (a)** shows a photograph of the fabricated antenna, and **Figure 38b** shows the comparison between measured and simulated reflection coefficient against frequency. It can be observed that measured results reasonably agree with the simulated ones for the proposed antenna and the bandwidth is about 225% (50–500 MHz) centered at 150 MHz. These frequencies are chosen at lower and higher frequencies in the pass band of this antenna, that is, at 50 and 500 MHz.

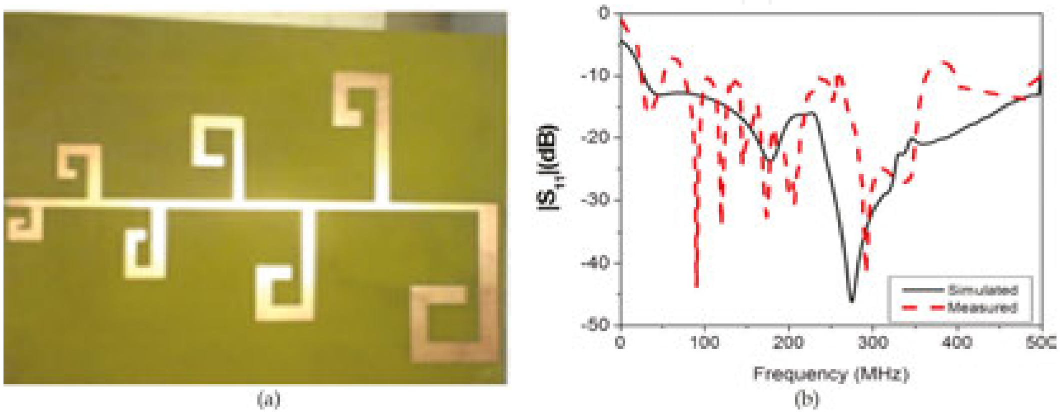

Figure 38. (a) Photograph of the fabricated antenna and (b) comparison between measured and simulated, reflection coefficient.

7. Conclusion

Three examples are given for nondestructive tests, namely noninvasive glucose monitory techniques for dielectrics, microwave bio-sensor for rapid detection of the viruses in biological, and the ground penetrating radar. The first example focuses on the possibilities of a monitor that noninvasively measures blood glucose levels using electromagnetic waves. The technique is based on relating a monitory antenna's resonant frequency to the permittivity and conductivity of skin which in turn is related to the glucose levels. The second applications is the use of biosensor for rapid detection of the enteroviruses which limits the need for sophisticated laboratory diagnostic methods that needs long time and expert scientists to perform the best. The physician in the field normally does fast and simple tests and then gives a fast decision regarded as potentially safe or not. The proposing micro-immunosensing diagnostic assay is based on the very specific immune reflection between antigen and its antibody. The third application is using the ground penetrating radar as a nondestructive test for identifying the underground targets. It consists of a transmitting antenna, which is used to transmit a signal to the ground depending on the received signal scattered from the buried body in the ground, identification of the underground target may take place. In our case, this technique was used for detecting underground water, which is very vital application for many countries nowadays.

Acknowledgements

Some results are done under the support of Egypt Science and Technology Development Fund, STDF, Egypt with contract number: 4149 and contact no. 3137.

Author details

Dalia M.N. Elsheakh*, Esmat A. Abdallah and Hala A. Elsadek

*Address all correspondence to: daliaelsheakh@gmail.com

Electronics Research Institute, Giza, Egypt

References

[1] D. Daneman, "Type 1 Diabetes." The Lancet, vol. 367, no. 9513, pp. 846–858, 2006.

[2] C. Ogden, C. Engelga, A. A. Hedley, M S Eberhardt, and S H Saydah. "Prevalence of Overweight and Obesity Among Adults with Diagnosed Diabetes – United States, 1988–1994 and 1999–2002." Morbidity and Mortality Weekly Report, November 19, pp. 1066–1068, 2004.

[3] H. Paul, T. Dall, and P. Nikolov. "Economic Costs of Diabetes in the U.S." Diabetes Care (American Diabetes Association), vol. 26, pp. 917–932, 2003.

[4] "Executive Summary: Standards of Medical Care in Diabetes—2010." Diabetes Care (American Diabetes Association), vol. 33, pp. S4–S10, 2010.

[5] M. David, J. Kuenen, B. Rikke, H. Zeng, D. Schoenfeld, and R. J Heine. "Translating the A1C Assay Into Estimated." Diabetes Care (American Diabetes Association), no. 31, pp.1–6, 2008.

[6] R. Francine, L. C Gibson, M. Halvorson, S. Carpenter, L. K Fisher, and P. Pitukcheewanont. "A Pilot Study of the Continuous Glucose Monitoring System." Diabetes Care (American Diabetes Association), no. 24, pp. 2030–2034, 2001.

[7] C. Leland, and C. Lyons. "Electrode Systems for Continuous Monitoring in Cardio vascular Surgery." Annals of the New York Academy of Sciences, vol. 102, pp. 29–45, 1962.

[8] D. Jeffrey, and A. P F Turner. "Home Blood Glucose Biosensors: A Commercial." Biosensors and Bioelectronics, vol. 20, no. 12, pp.2435–2453, 2005.

[9] T. Andrea, A. Maran, and G. Pacini. "Non-invasive Glucose Monitoring: Assessment of Technologies and Devices According to quantitative criteria." Diabetes Research and Clinical Practice, no. 77 pp. 16–40, 2007.

[10] G. Dongman, D. Zhang. "Monitor Blood Glucose Levels via Breath Analysis System and Sparse Representation Approach." IEEE Sensors Conference, Nov. pp.1238–1241, Kona, HI 2010.

[11] M.Yuki, T. Horiguchi, H. Ishizawa, S.Tezuka, H.Hara. "Basis Examination for Development of Noninvasive Blood Glucose Measuring Instrument by Near-Infrared Confocal Optical System." SICE Annual Conference, Taipei, Taiwan, 2010.

[12] L.Kirill, M. Eledrisi, M. Motamedi, R. Esenaliev, "Noninvasive Blood Glucose Monitoring with Optical Coherence tomography: a pilot study in human subjects." Diabetes Care (American Diabetes Association), 25, no. 12, pp. 2263–2267, 2002.

[13] Yeh, Shu-Jen, Chrales Hanna, Omar Khalil, "Monitoring Blood Glucose Changes in Cutaneous Tissue by Temperature-Modulated Localized Reflectance Measurements." Clinical Chemistry, vol. 49, no. 6, pp.924–934, 2003.

[14] C. Green, and R. Jean, "Design of a Microwave Sensor for Non-Invasive Determination of Blood-Glucose Concentration." Master's Thesis, Engineering and Computer Science, Baylor University, 2005.

[15] B. Randall, E. C Green, and M. J McClung. "A Microwave Frequency Sensor for Non-Invasive Blood-Glucose." IEEE Sensors Applications Symposium, Atlanta, GA, 2008.

[16] M. Yvanoff and J Venkataraman. "A Feasibility Study of Tissue Characterization Using LC Sensors." IEEE Transactions on Antennas and Propagation, vol. 57, no. 4, pp. 885–893, 2009.

[17] J. Jung, W. Choi ; J. Choi, "A Small Wideband Microstrip Fed Monopole Antenna." IEEE Microwave and Wireless Components Letters , vol.15, pp. 703–705, Oct., 2005.

[18] J. Yves, N. Le Prieur, L. Campion, I. Guilhem, H. Allannic, and D. Maugendre. "Clinical and Statistical Evaluation of Self-Monitoring Blood Glucose Meters." Diabetes Care(American Diabetes Association), vol. 21, no. 11, pp.1919–1924, 1998.

[19] G.L. Dai and M.Y. Xia, "Design of Compact Dual-Band Switchable Bandpass Filter", Electron Letters, vol. 45, pp. 506–507, 2009.20. "ADF4350 Data Sheet Rev. 0." Analog Devices. 2008. http://www.analog.com/static/ imported-files/data_sheets/ADF4350.pdf.

[20] D.Elsheakh and E.Abdallah, "Novel Rapid Detection of Different Viruses in blood Using Microimmuno-Sensor", The 7th European Conference on Antennas and Propagation (EuCAP) 8–12 April in Gutenberg, Sweden, 2013.

[21] "Agilent 85070E Dielectric Probe Kit: Technical Overview." Agilent Technologies. March 28, 2008. http://cp.literature.agilent.com/litweb/pdf/5989-0222EN.pdf

[22] D. Pozar, "Microwave Engineering", 4th ed. John Wiley & Sons, Inc, 2012

[23] S. Gabriel, et al. "The Dielectric Properties of Biological Tissues: II. Measurements in the Frequency Range 10 Hz to 20 GHz." Physics in Medicine and Biology, pp. 2231–2250, vol. 41, no.11.

[24] D. Elsheakh, H. A. Elsadek, E. A.Abdallah, S. Atteya, and W. N. ELmazny, " Rapid Detection of Blood Entero-Viruses Using Microstrip Antenna Bio Sensor", The 16th European Microwave Week, Germany, 2013.

[25] K.S. Cole and R.H. Cole, "Dispersion and Absorption in Dielectrics – I Alternating Current Characteristics". The Journal of Chemical Physics, vol. 9, pp. 341–352. Bibcode 1941JChPh…9..341C.doi:10.1063/1.1750906.

[26] J.H. Park, et al., "The Correlation of the Complex Dielectric Constant and Blood Glucose at Low Frequency." Biosensors and Bioelectronics, vol. 19, no. 4, pp. 321–324, 2003.

[27] Y. Rahmat-Samii, "Wearable and Implantable Antennas in Body-Centric Communications," Antennas and Propagation, 2007. EuCAP 2007. The Second European Conference, pp.1–5, 11–16, Nov. 2007.

[28] T. Chen, D. Dubuc, K.Grenier, "Resonant-Based Microwave Biosensor for Physiological Liquid Identification," 42nd European Microwave Conference (EuMC), pp. 448,450, 2012.

[29] D. Elsheakh and E. Abdallah, "Novel Rapid Detection of Different Viruses in blood Using Microimmuno-Sensor", The 7th European Conference on Antennas and Propagation (EuCAP), 8–12 April in Gutenberg, Sweden, 2013.

[30] D.Elsheakh, H. A. Elsadek, E. A. Abdallah, S. Atteya, and W. N. ELmazny, " Rapid Detection of Blood Entero-Viruses Using Microstrip Antenna Bio Sensor", The 16th European Microwave Week, Germany, 2013.

[31] P. Debye, "Polar Molecules," Dover Publications, Mineola, NY, 1929.

[32] M. Pieraccini, A. Bicci, D. Mecatti, G. Macaluso, C. Atzeni, "Propagation of Large Bandwidth Microwave Signals in Water," IEEE Antennas and Propagation Society, vol. 57, no. 11, pp. 3612–3618, 2009.

[33] D. N. Elsheakh and E. A. Abdallah, "Ultra Wide Band Planar Printed Quasi-Yagi Antenna with Size Reduction for Water Detection in the Egyptian Desert", Microwave and Optical Technology Letters, vol. 57, no. 1, pp.226–233, 2015.

[34] D. N. Elsheakh and E.A. Abdallah, "Compact Shape of Vivaldi Antenna for Water Detection by Using Ground Penetrating Radar (GPR)", Microwave and Optical Technology Letters, vol. 56, no.8, pp. 1801–1809, 2014.

[35] D. Elsheakh and E. A. Abdallah, "Compact Printed Log-Periodic Dipole Antenna for Water Detection by Using Ground Penetrating Radar (GPR)", Microwave and Optical Technology Letters, vol. 56, no. 6, pp. 1225–1232, 2014.

[36] X. X. Yin et al., "A Resistive Loaded Tapered Slot antenna for Ground Penetrating radar", Modern Radar, vol. 28, pp. 58–68, 2006.

[37] K., Tutku, A. Hood, and E. Topsakal. "Design of a Dual-Band Implantable Antenna and Development of Skin Mimicking Gels for Continuous Glucose Monitoring." IEEE Transactions on Microwave Theory and Techniques vol. 56, no. 4, pp. 1001–1008, 2008.

[38] K. Buell, H. Mosallaei, and K. Sarabandi, "Metamaterial Insulator Enabled Superdirective Array," IEEE Antennas and Propagation Society, vol. 55, no. 4, pp. 1074–1085, 2007.

IntechOpen